4. RESULTS AND DISCUSSIONS

4.1 Nanosuspensions for inhalation. Development and nebulization behaviour

4.1.1 Development, follow up stability and dissolution studies of buparvaquone nanosuspensions

4.1.1.1 Optimisation of the number of homogenisation cycles

The buparvaquone crystalline powder as received had LD d50% of 86.5 ± 9.0 µm and d99% was 465.1 ± 24.4 µm. As it has been deeply discussed by Müller and co-workers, the mean particle size in the nanometer range obtained by high pressure homogenisation depends on the pressure applied, the number of homogenisation cycles and the hardness of the drug itself. For each drug, a minimum size exists and can be achieved by applying a certain pressure (i.e. power density in the homogeniser) (Müller, Jacobs et al. 2001). In conventional piston-gap homogenisers for lab scale production (e.g. APV Gaulin Micron LAB 40 used in this work), only homogenisation pressures from 100-1500 bar can be applied (Müller and Böhm 1998), which is the applicable pressure range for pharmaceutical production. Higher pressures are technically possible, but lead to a high wearing of the machines. This is rather an exponential than a linear relationship between increased wearing and increased pressure. Therefore, for the production of aqueous buparvaquone nanosuspensions prepared in this work, a pressure of 1500 bar was applied and the optimum number of cycles was investigated in order to achieve maximum homogeneity and minimum nanocrystal size. The homogenisation process was followed up to 60 cycles. The typical profile of the values measured with LD is shown with a representative batch in Figure 4-1. These results were obtained homogenising a 1% drug nanosuspension in aqueous dispersion medium. The d50% decreased markedly at the beginning of the homogenisation process, yielding particles with a diameter of 0.656 µm after 10 cycles. Increasing the cycle number to 60 only led to a small decrease to 0.427 µm. In contrast to the LD d50%, showing only limited further decrease after cycle 25, the benefit of applying higher cycle numbers is clearly seen when looking at the LD diameters d90%, d95% and d99%. There is a further pronounced decrease when increasing the number to 40 cycles. The LD d99% was reduced to 5.870 µm after 5 homogenisation cycles and to 1.443 µm after 40 cycles. The mean diameter of the entire population measured by PCS showed practically no

change after 40 cycles, similar to this the LD 50% measured by laser diffractometry showed also little change. For the diameters LD d90% to LD d99% there was no further reduction when moving from 40 cycles to 60 homogenisation cycles. The LD d99% decreases from 1.443 µm after 40 cycles to 1.442 µm after 60 cycles. This effect can be explained by the increasing hardness of the crystals with decreasing crystal size. Breaking of the crystals takes place preferentially at the imperfections, with decreasing size the number of imperfections decreases, that means the crystals are getting more and more perfect. Reaching a certain minimum size and related crystal hardness, the power density given at the applied homogenisation conditions is not high enough for further crystal diminution, as it has been described before for this kind of formulations.
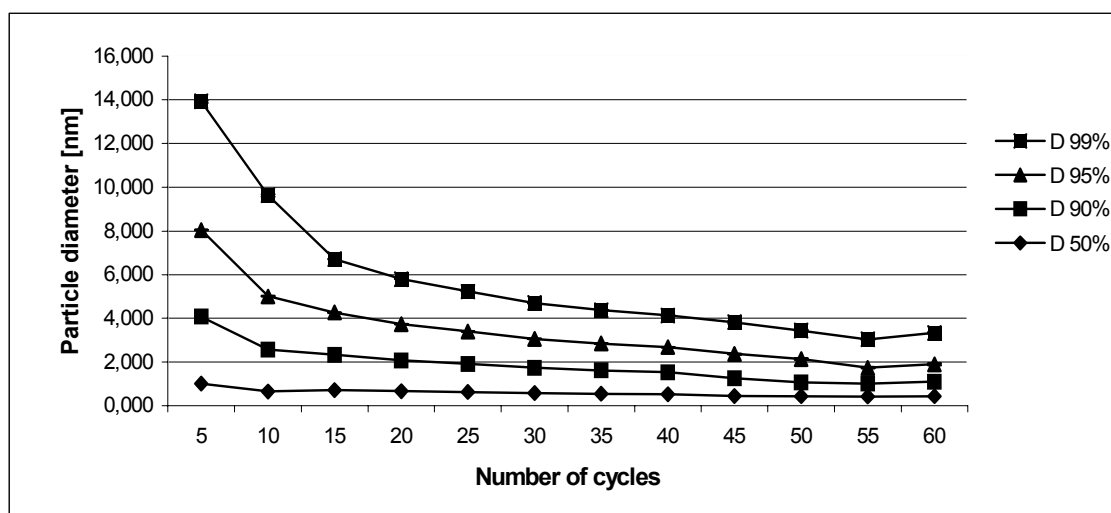

Figure 4-1: LD diameters d50%, d90%, d95% and d99% obtained along a 60 cycles homogenisation process at 1500 bar. Dispersion medium is an aqueous solution of 0.5% poloxamer 188.

The Figure 4-2 represents the data obtained with PCS technique along the 60 homogenisation cycles. The average diameter of the drug nanocrystals measurements improved from 721.5 nm (polydispersity index PI=0.45) to 494.3 (PI=0.34) after 15 homogenisation cycles. A further improvement was seen after 40 cycles when the average particle size obtained was 403.0 nm (PI= 0.23), meaning a more homogeneous suspension. An average diameter of 339.1 (PI=0.23) was obtained after cycle 60, supporting the results already seen with LD. Based on these results, it was decided to produce buparvaquone nanosuspensions with 40

homogenisation cycles to obtain optimized size and homogeneity of the nanosuspensions.
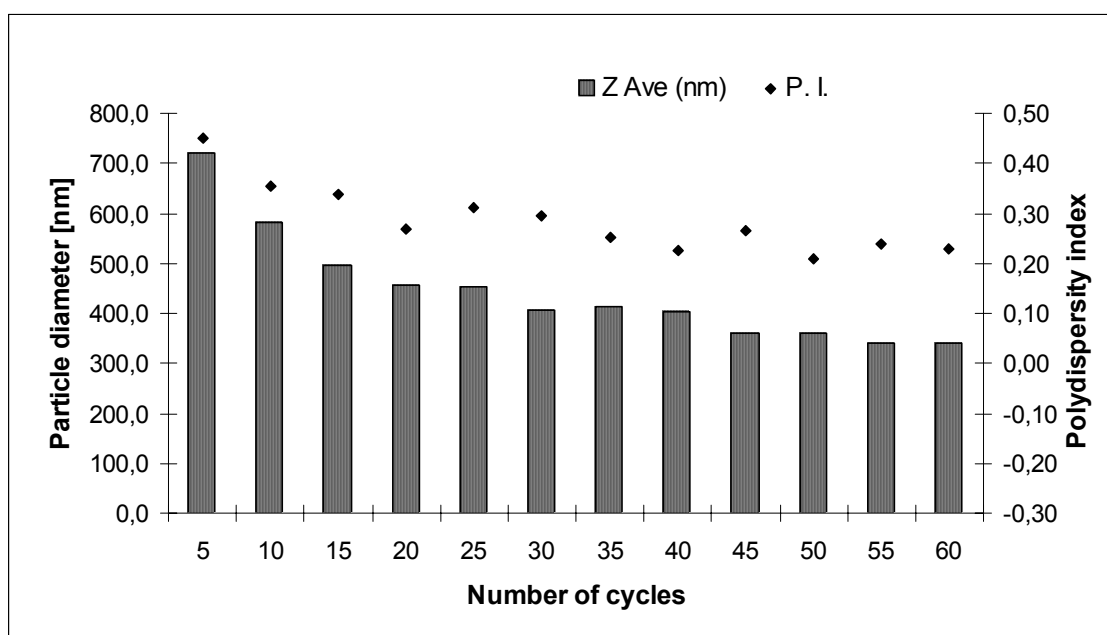

Figure 4-2: Z-Average and polydispersity index (PI) values obtained with PCS along a 60 cycles homogenisation process at 1500 bar. The dispersion medium is an aqueous solution of 0.5 % poloxamer 188.

4.1.1.2 Formulation screening with different dispersion media and follow-up stability
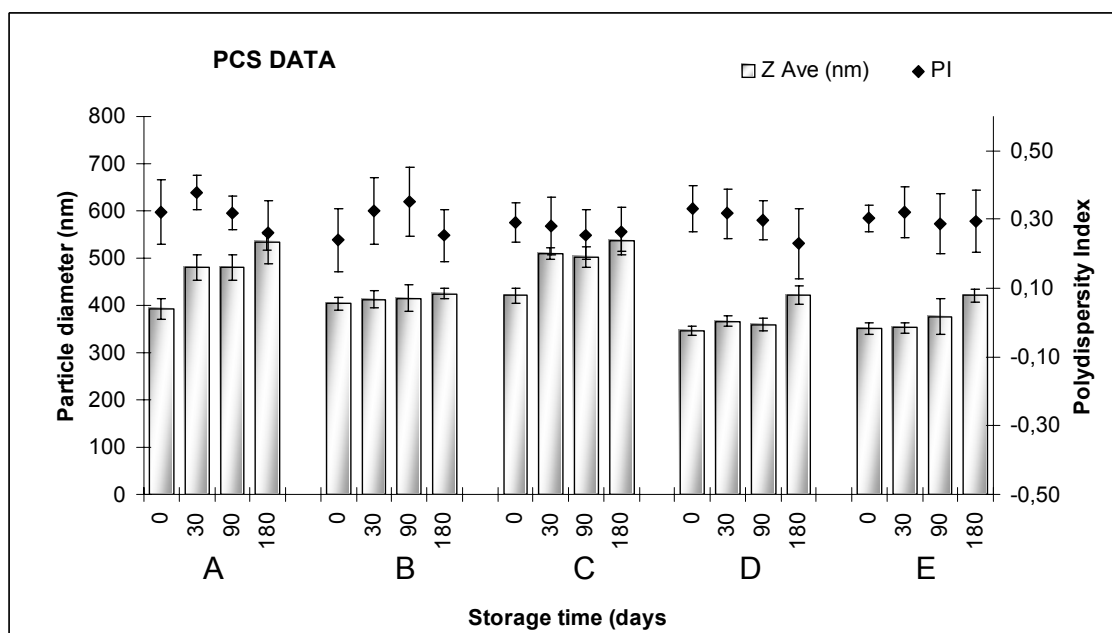
The homogeneity of the drug nanocrystal size distribution after the homogenisation process will be a decisive factor in the long-term stability of the formulation. Additionally, the physical interaction between the drug molecules and the surfactant used to avoid nanocrystal aggregation will also determine the stability of the suspension. The application and route of administration of the nanocrystals prepared and the composition of the formulation, i.e. the regulatory status of the excipients, were considered in this work to select the best formulations to be candidate for pulmonary application in aqueous droplets. The composition of the nanosuspensions prepared for the screening are described in Table 4-1.

Table 4-1: Formulation composition of the nanosuspensions prepared for pulmonary administration
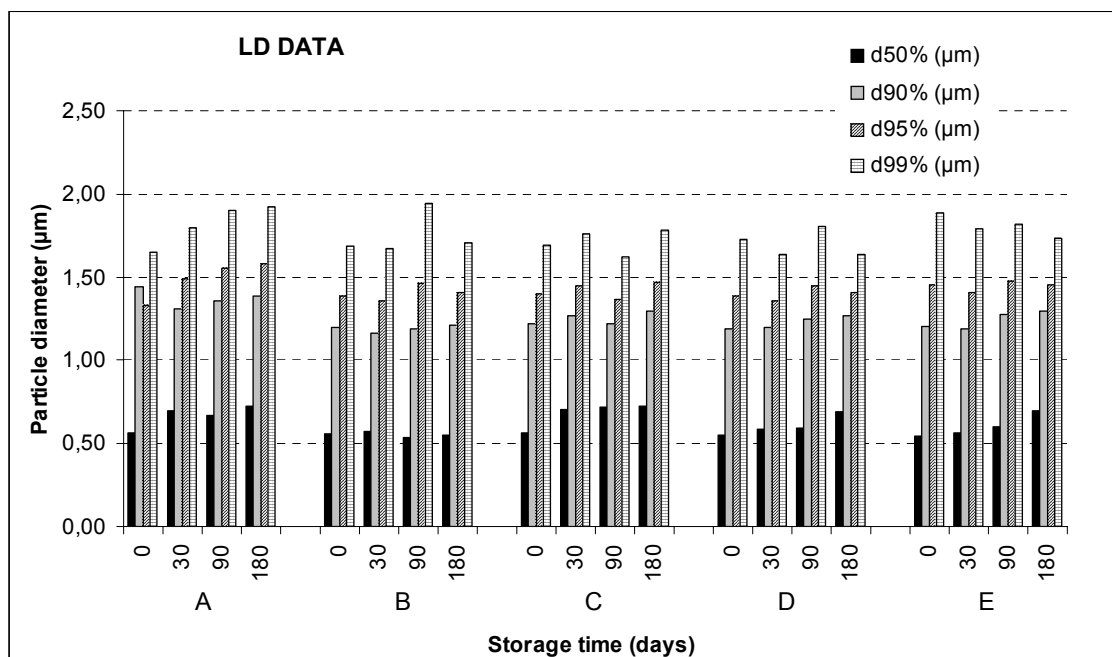
FORMULATION	COMPOSITION (% w/w)*
A	1 % BPQ (1 % Polox. 188)
B	1 % BPQ (0.5 % Polox. 188 + 0.5 % PVA)
C	1 % BPQ (0.5 % Polox. 188 + 0.5 % Phospholipon 80 + 0.3 % sodium glycocholate)
D	1 % BPQ (0.3 % Tyloxapol)
E	1 % BPQ (0.5 % Polox. 188 + 0.15 % Tyloxapol)
F	2 % BPQ (0.5 % Polox. 188 + 0.15 % Tyloxapol)
G	7 % BPQ (0.5 % Polox. 188 + 0.15 % Tyloxapol)
H	1 % BPQ (1 % Phospholipon 90G)
I	1 % BPQ (0.5 % Tween 80)
J	1 % BPQ (1.0 % Tween 80)
K	1 % BPQ (2.0 % Tween 80)

* All formulations contain 2.5 % Glycerol 85 % in order to adjust the osmolarity and water was added to complete a 100 % of the composition indicated.

The size distribution of the drug nanocrylstals was followed up during 6 months using LD and PCS techniques. The Figure 4.3 represents the LD and PCS diameters obtained at day 0, 30, 90 and 180 after preparation for formulation A to E. All formulations contain 1 % of drug content. The formulation containing PVA (B) as well as those containing tyloxapol (D and E) have shown almost no difference in the particle diameter measured by PCS. Formulations A and C showed a slight increase of about 100 nm within 6 months, with approximately constant values in polydispersity index. This increment was not considered critical, as the LD particle diameter values d50%, d90%, d95% and d99% confirmed the absence of big aggregates or larger microparticles after 6 months of storage. These formulations were considered appropriate for the use in nebulizers considering that the LD diameter d99% was below 2 µm in all the cases. The size diameter of aqueous droplets produced by most of the nebulizers offered nowadays in the market is equal or bigger than 2 µm, and therefore the nanosuspensions A-E were considered appropriate to be incorporated in wet aerosols using nebulizers.

(a)

(b)

Figure 4-3: Particle size distribution of the drug nanocrystals in formulations A-E measured at the day of production and after 1, 3 and 6 months of storage time at room temperature. Size distribution was measured with PCS (a) and LD (b) techniques.

The possibility to deliver high doses of drug directly to the lung is one of the interesting issues using nanosuspensions through nebulization. Due to high pressure homogenisation, higher concentrations of drug than 1 % will also yield products with low viscosity and density, easier to be nebulized than conventional suspensions. In order to investigate the stability of higher concentrated suspensions, the surfactant composition of formulation E was selected and the content of drug was increased to 2 and 7 % using the same surfactant mixture (formulations E-G). The resultant particle size distribution along 6 months can be seen in Figure 4-4a and Figure 4-4b. A negligible increment in the PCS particle diameter was observed, while the polydispersity index value remained unchanged. LD diameters were also considered satisfactory, confirming the absence of drug nanocrystal aggregates or the formation of larger crystals.
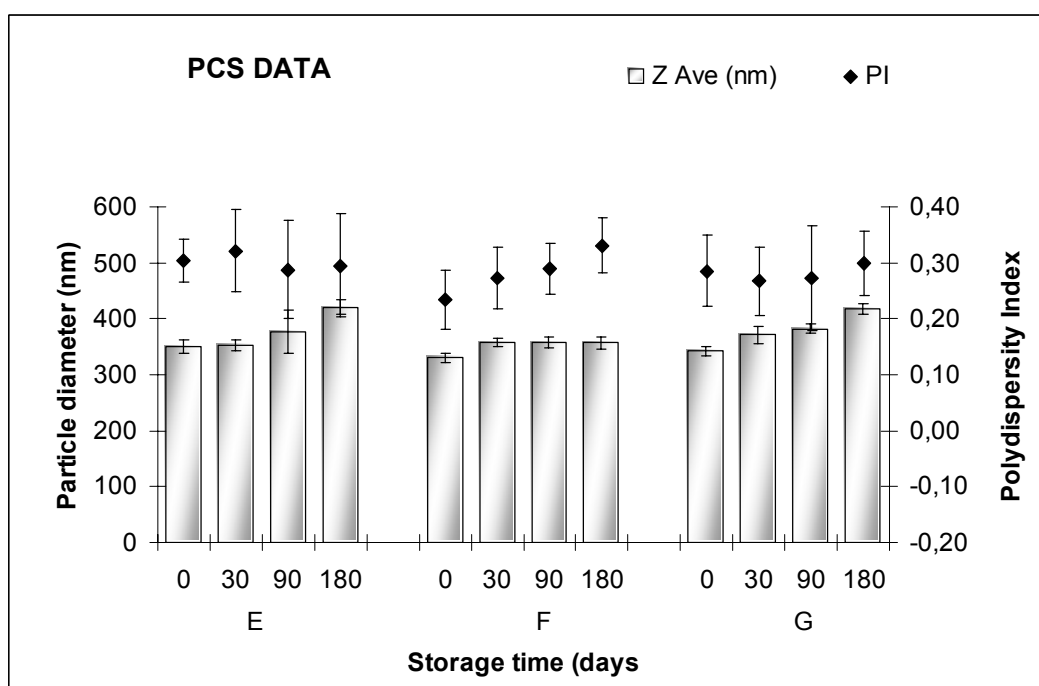

Figure 4-4a: Z Average particle diameter and polydispersity indices measured with PCS technique. Formulations E, F and G contain 1, 2 and 7 % of drug respectively.
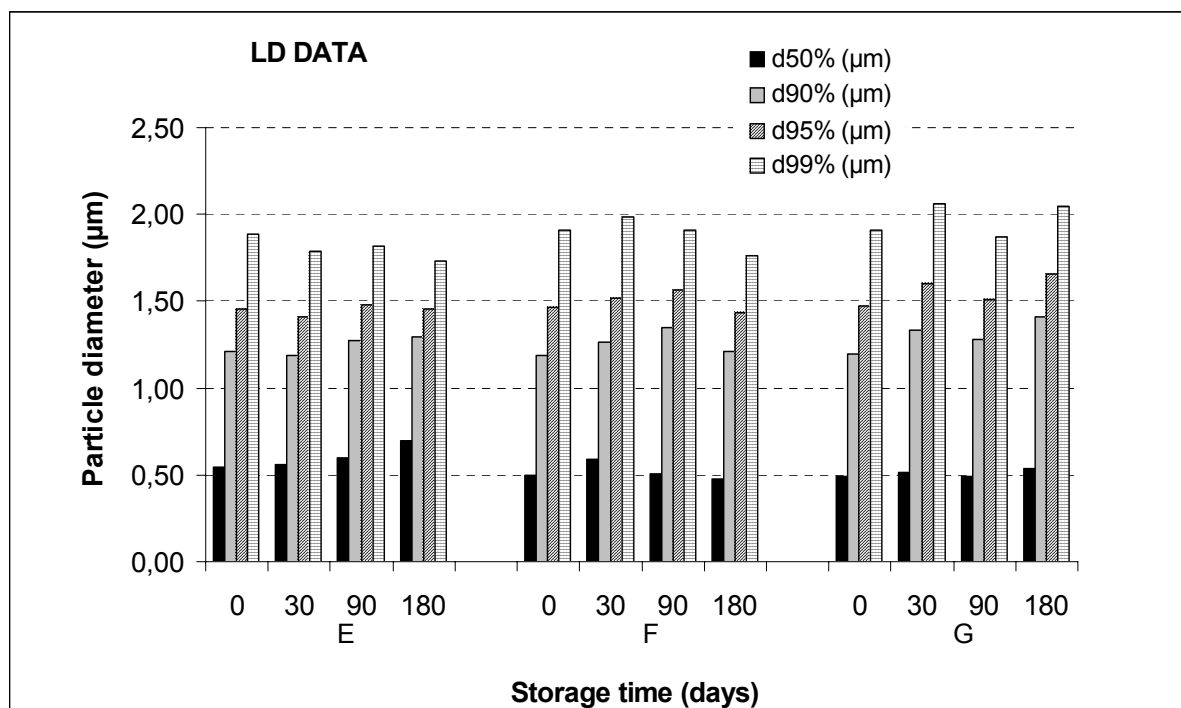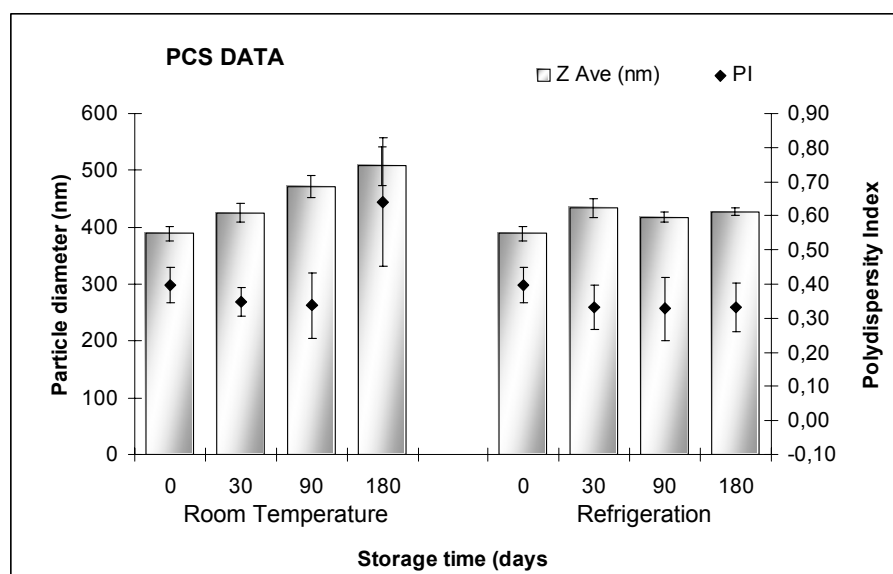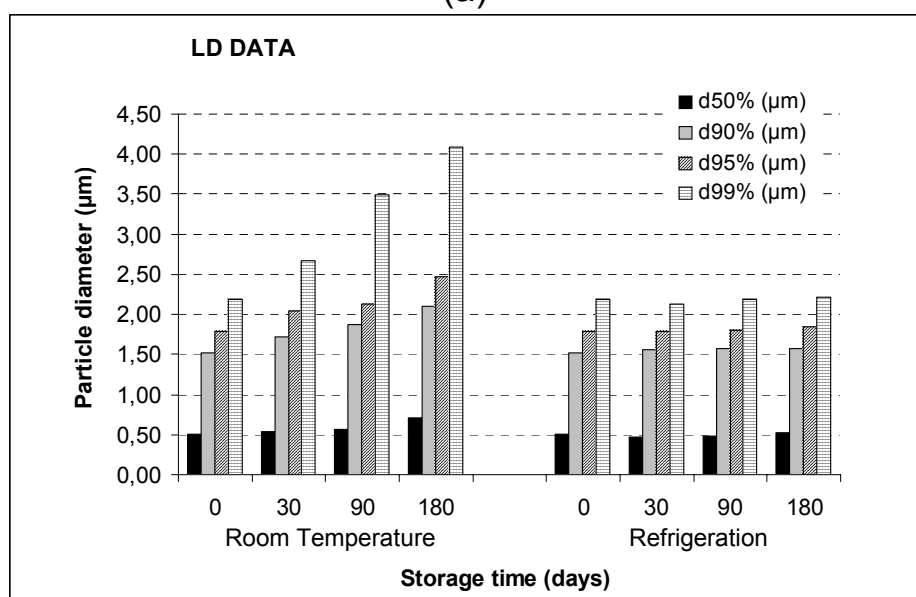
Figure 4-4b: LD particle diameter measured for formulations E, F and G contain 1, 2 and 7 % of drug respectively along 6 months storage time.

The use of phospholipids in pulmonary formulations has become relatively usual. Phospholipids are the primary natural component of cell membranes and thus of the surfaces available for absorption in the lung. Natural lung surfactants consists by 80-90% of lipids, of which phosphatidylcholine makes 70 to 80% (McAllister, Alpar et al. 1996). The results of stabilizing BPQ nanocrystals using soja lecithin (formulation H) and the follow up stability study within 6 months are shown in Figure 4-5. Samples were stored at room temperature and under refrigeration (5 ± 3 °C). At room temperature, nanocrystal growth was observed by PCS. Although the average particle diameter increased only around 100 nm, the polydispersity index increased from 0.4 to 0.7 after 6 months. Also LD measurements showed particle diameters d99% increasing from 2 to 4 μm. The presence of aggregates was confirmed microscopically. As is well known, reducing the storage temperature can conduct to a reduction of particle aggregation and to an improvement of the formulation stability (Böhm 1999). A reduction in the temperature of the dispersion medium increases the viscosity of the phospholipid dispersion reducing the diffusion coefficient of the particles according to Stokes-Einstein Equation. A reduction of the diffusion coefficient consequentially slows the diffusion of the nanocrystals according to

Fick'schen Law. A reduction in the probability of collision between particles is reduced in this manner. Formulations stored under refrigeration were stable within the 6 months evaluated (see Figure 4-5).

(a)

(b)

Figure 4-5: Particle size distribution of the drug nanocrystals in formulation H measured at the day of production and after 1, 3 and 6 months of storage time at room temperature and under refrigeration. Size distribution was measured with PCS (a) and LD (b) techniques.

Less stable formulations were those prepared using Tween® 80 as stabilizer. The Figure 4-6 represents the following up stability study of formulation I to K within 6 month storage at room temperature. A surfactant increment to a concentration of 2 % avoided the presence of nanocrystal aggregation, as it can be seen in LD measurements. However, the PCS values for formulation K shows a constant increment in the particle diameter, which indicates instability of the dispersion.
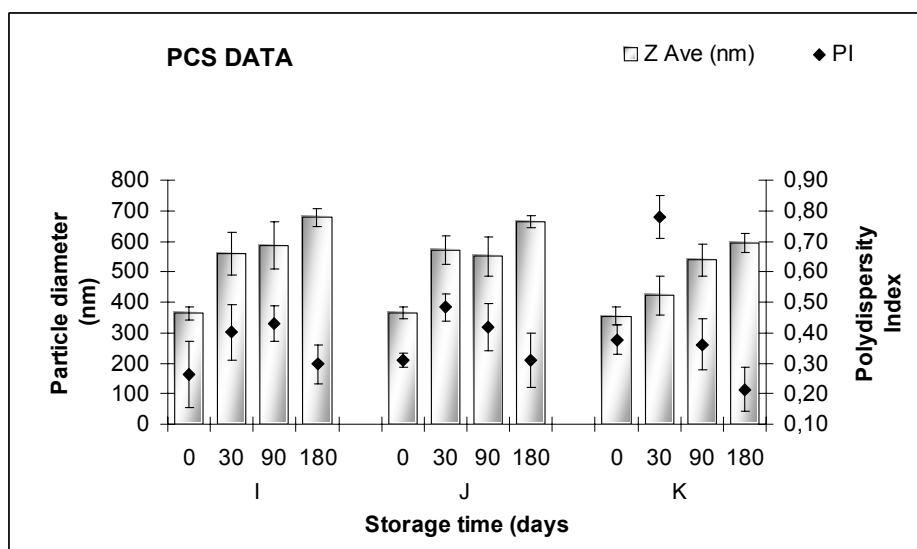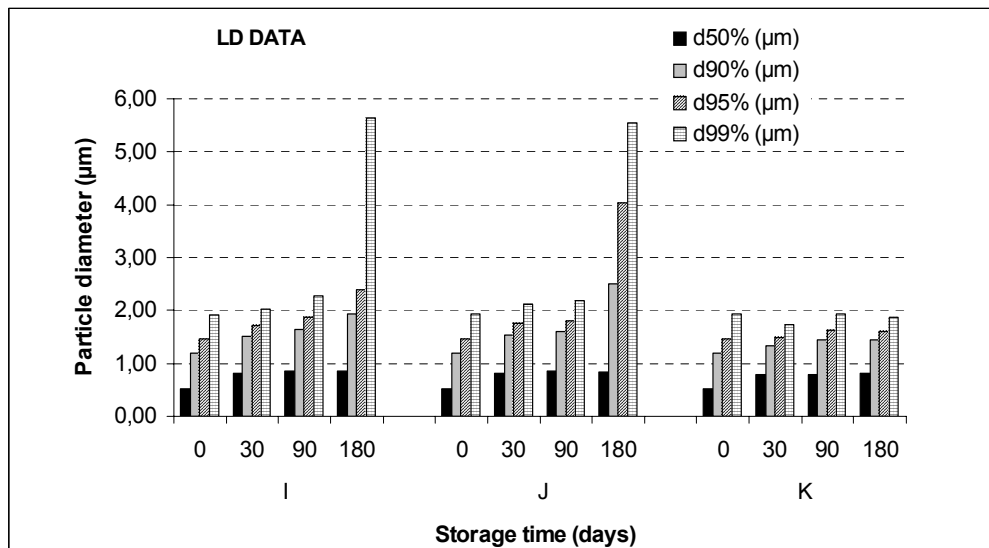

(a)

(b)

Figure 4-6: Particle size distribution of the drug nanocrystals in formulations I-K measured at the day of production and after 1, 3 and 6 months of storage time at room temperature. Size distribution was measured with PCS (a) and LD (b) techniques.

The size distribution data obtained at the time of production and up to 6 months stability with LD and PCS techniques can be seen in Appendix A.

Physical instability then leads to a size increase either by crystal growth due to Ostwald ripening or alternatively due to aggregation caused by insufficient stabilization. The nanosuspensions were stabilized by different surfactants, most of them non-ionic type (see section 3.1.4), sterically stabilizing excipients. In addition, the electrostatic repulsion contributes to the stabilization, in this case it is a combined effect. A measure for the electrostatic repulsion is the zeta potential. Table 4-2 resumes the zeta potential values of the formulations prepared.

Table 4-2: Zeta potential values for the buparvaquone nanosuspensions selected due to their good stability. Measurements were performed in adjusted 50 µS/cm Milli-Q water and at pH 6.0-7.0

FORMULATION	Z POTENTIAL (mV)
A	-26.0 ± .0.7
B	-9.1 ± 0.7
C	-46.6 ± 0.2
D	-46.6 ± 1.2
E	-46.8 ± 0.8
F	-46.8 ± 1.7
G	-40.6 ± 1.7
H	-35.4 ± 1.0

Under the measuring conditions, the zeta potential is mainly a function of the particle surface charge (Nernst potential). A good physical long-term stability of the dispersion is normally predicted by a zeta potential higher than +30 mV or lower than -30 mV (Riddick 1968). Although formulations A and B showed low zeta potential values, the sterically stabilizing effect of the surfactant chains resulted in acceptable long-term stability.

Additional to the physical stability of the formulations prepared, a quantification using HPLC technique was performed simultaneously in order to detect possible degradation of the drug. All formulations with good physical stability (Formulations A-

H) showed excellent stability of drug content within the time investigated (6 months). A summary of the drug contents determined in the formulations is given in Table 4-3.

Table 4-3: Drug content of physically stable nanosuspension formulations at the day of production and after 6 months of storage. Measurements performed with HPLC method. Values represent the mean ± SD of 3 measurements.

FORMULATION	CONTENT AT DAY 0 (mg/mL)	CONTENT AT DAY 180 (mg/mL)
A	11.5 ± 0.9	10.4 ± 0.6
B	9.11 ± 0.8	9.0 ± 0.9
C	10.5 ± 0.7	10.0 ± 0.5
D	11.6 ± 0.9	10.5 ± 0.6
E	10.1 ± 0.8	9.7 ± 0.8
F	21.0 ± 2.1	20.3 ± 0.9
G	69.9 ± 3.1	70.2 ± 0.5
H*	10.0 ± 0.9	10.2 ± 0.7

*Formulation stored under refrigeration

4.1.1.3 Crystallinity of the nanosuspensions

The Figure 4-7 shows the SEM photographs of buparvaquone bulk powder (upper) and buparvaquone after 40 homogenisation cycles (lower) in aqueous dispersion medium.
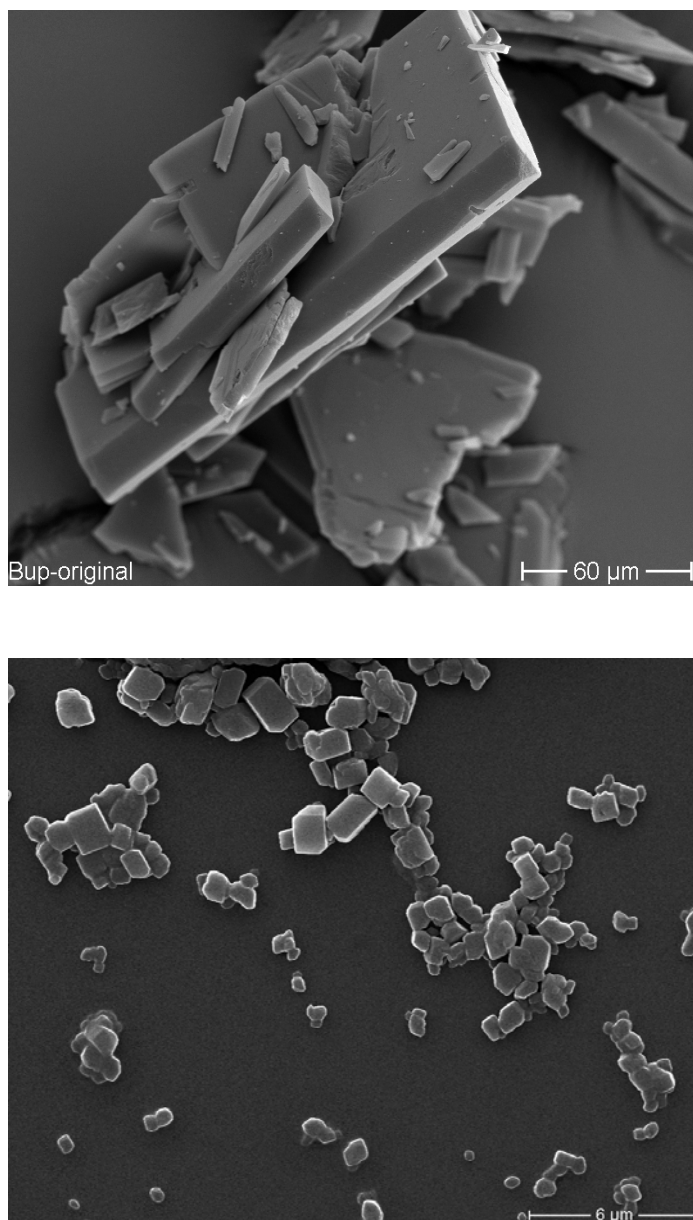

Figure 4-7: SEM Photographs of buparvaquone original (upper) and nanosuspension after 40 homogenisation cycles (lower). Homogenisation at 1500 bar, room temperature.

The original drug consists of big, flat, sharp-edged crystals. After the high pressure homogenisation process, the small nanoparticles are not only small, but also have a nice cubic shape. The presence of very few microcrystals within the range of 1-1.5 µm was also confirmed with this technique, supporting the results previously observed with LD and polarized light microscopy.

The Figure 4-8 represents the X-Ray diffractogram of the buparvaquone nanosuspension formulation H after 5 (a) and 40 (b) homogenisation cycles.

The diffractogram obtained from a placebo formulation is also shown (c). It can be seen that as the number of homogenisation cycles increases, it will also increase the disorder of the crystal lattice, shown here as a decrease in peak intensities due to the formation of a partially amorphous structure. The X-Ray pattern of the drug is still recognizable after 40 homogenisation cycles, but its peak intensities are clearly reduced due to the process.
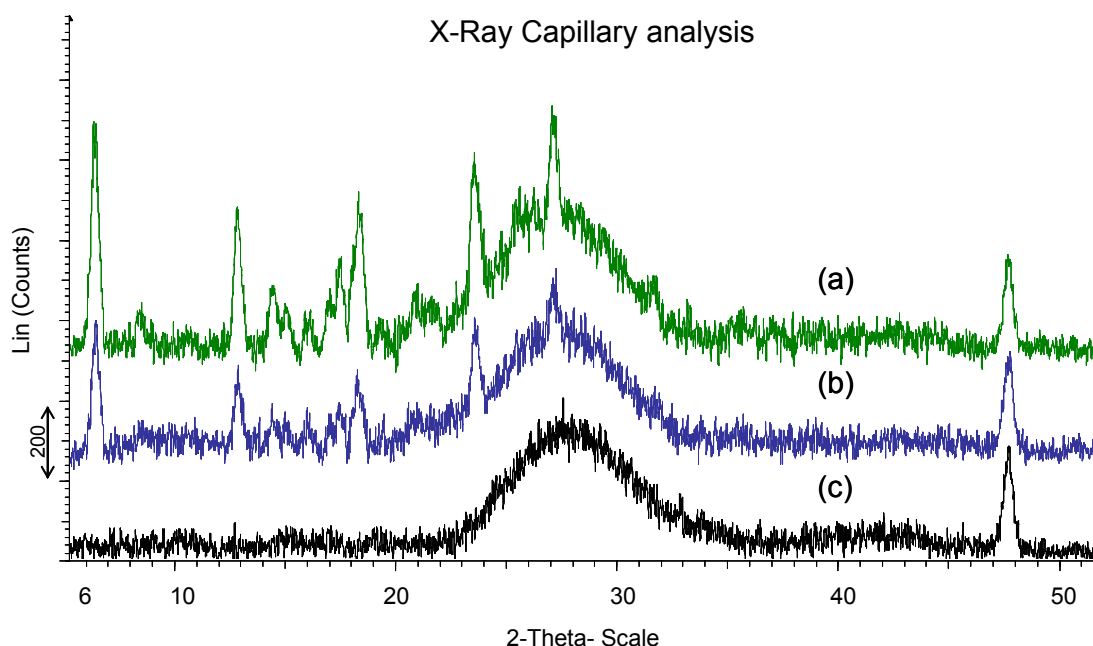

Figure 4-8: X-Ray diffractogram of aqueous buparvaquone nanosuspension formulation H (Phospholipon 90G formulation) after 5(a), and 40 (b) homogenisation cycles. A placebo formulation is shown in (c). Capillary sample holder was used for the measurement of the aqueous dispersion.

4.1.1.4 Saturation solubility of buparvaquone nanocrystals

The saturation solubility of buparvaquone nanocrystals was determined after 1 week of preparation and measured with HPLC. During this week, the nanosuspensions were kept in a temperature controlled shaking cupboard (25 °C, 120 rpm). 1 mL of each formulation were placed in each one of 2 Eppendorf tubes. Then, ultracentrifugation at 17,000 rpm was repeated 2 times, 1 hour each. The table 4-4 shows the results obtained for the formulations in discussion.

Table 4-4: Saturation solubility values for the buparvaquone nanosuspensions selected. Measurements were performed using HPLC method. PCS particle diameters of the drug nanocrystals are also summarized.

FORMULATION	SATURATION SOLUBILITY (µg/mL)	PCS Particle diameter (nm)
A	0.33	392.3 ± 22.4
B	0.34	403.9 ± 13.8
C	2.56	420.9 ± 16.8
D	1.04	345.3 ± 0.33
E	1.15	350.7 ± 12.8
F	1.14	330.7 ± 8.4
G	0.72	342.4 ± 8.5
H	2.07	388.7 ± 13.4

The aqueous solubility of buparvaquone has been reported to be < 0.03 µg/mL. As it can be seen in Table 4-4, the saturation solubility of the drug nanocrystals have increased through the formulation. The solubility values are at least ten-fold higher than the original value reported in only water and in some cases, when phospholipids were present in the formulation, even higher.

4.1.1.5 *In vitro* dissolution behaviour of buparvaquone nanocrystals

In vitro dissolution tests of nanosuspensions performed as described in section 3.2.2.9 were carried out with BPQ nanocrystals. The average particle diameters of the nanocrystals were 400 nm, 700 nm and 1.5 µm (all LD d50% diameters). The Figure 4-9 represents the dissolution behaviour observed.

Figure 4-9: Dissolution test of buparvaquone nanocrystals and original powder (LD d50% = 86.5 ± 9.0 µm) using 2 %Tween 80 solution as a dissolution medium

Under the same dissolution conditions, only 3% of the drug powder were dissolved after 1 hour, and 11 % after 5 hours. The increase on the rate of dissolution of the drug proportional to the increase of the surface area in contact with the dissolution media could be confirmed by reducing the particle size of the drug nanocrystals. The 90% of the drug was dissolved within 12 minutes when the drug had an average diameter of 400 nm.

4.1.2 Nebulization performance

4.1.2.1 Droplet size in aerosols

In a first basic study (Hernández-Trejo, Kayser et al. 2005) four different nebulizers were used for the nebulization of two drug nanosuspension formulations (A and B). The nebulizers employed were described previously in Table 3-1 (see section 3.1.5.5). The droplet size of the generated aerosol was analyzed using a Sympatec laser diffractometer according to the method described in section 3.2.3.2. Two different nanosuspension formulations were nebulized to study a potential effect of the formulation itself on the nebulization performance. Table 4-5 shows the composition of the two formulations and the dispersion solutions used as references for comparison. In addition, the most suitable nebulizer for the nanosuspension should be identified.

Table 4-5: Composition of buparvaquone nanosuspension A and B used for nebulization study (after (Hernández-Trejo, Kayser et al. 2005)).

Formulations	Buparvaquone (% w/w)	Poloxamer 188 (% w/w)	Polyvinyl Alcohol (% w/w)	Glycerol 85% (% w/w)
Formulation A	1.0	1.0	--	2.5
Formulation B	1.0	0.5	0.5	2.5
Reference 1	--	--	--	2.5
Reference 2	--	0.5	0.5	2.5
Reference 3	--	1.0	--	2.5

The particle size characteristics of the drug nanosuspensions A and B compared in this work, measured before nebulization are listed in Table 4-6. The average diameter of the particles produced was around 400 nm (measured by photon correlation spectroscopy), while the 99% of the particles produced were under 2.6 μm (volume distribution values, measured by laser diffractometry). These are considered suitable sizes to be incorporated in aerosol droplets produced with an appropriate size to reach the alveolar spaces in the lung (1-3 μm) as it has been discussed in section 4.1.1.

Table 4-6: Particle size characterization (mean ± SD, n=3) of buparvaquone nanosuspension A and B used for nebulization study (after (Hernández-Trejo, Kayser et al. 2005)).

Parameter	Formulation A	Formulation B
PCS average diameter (nm)	473 ± 15	406 ± 8
PCS Polydispersity Index	0.34 ± 0.01	0.25 ± 0.05
d50% (µm)	0.92 ± 0.00	0.79 ± 0.01
d90% (µm)	1.56 ± 0.07	1.47 ± 0.08
d99% (µm)	2.58 ± 0.28	2.51 ± 0.30
Zeta potential (mV) (adjusted distilled water 50 µS/cm, pH 6)	-26.0 ± 0.7	-13.0 ± 0.2

Both formulations showed physical stability for at least 6 months as it has been shown in section 4.1.1. No crystal growth due to Ostwald ripening or aggregation was observed within that time. In general terms, low zeta potential values (< ±30 mV) are predictors of unstable formulations. However, the surfactants used to stabilize these nanosuspensions are non-ionic (see Table 4-1) and therefore a combined stabilization effect occurs with the investigated nanocrystals (steric plus electrostatic). The charge density on the surface of the particles leads to a certain electrostatic stabilisation of the dispersion. The low zeta potential values exhibited by these nanocrystals (-26.0 ±0.7 and -13.0 ±0.2) is due to steric stabilisation (mechanical barrier, shifts of plane of shear).

Theoretically there can be a difference when nebulizing a solution compared to the nebulization of a nanosuspension, despite the drug nanocrystals are ultrafine in size. Therefore the stabilizer solutions (= dispersion medium of the drug nanocrystals) were also nebulized as a reference.

Figure 4-10 (top) shows exemplarily the characterization diameters of the drug nanosuspension A and the pure stabilizer solution being nebulized by Respi-jet Kendall nebulizer. The droplet size distribution is practically identical, in this case the

presence of the nanocrystals had no effect on the nebulization result. An effect was observed with drug nanosuspension A when using the nebulizer Pari Turbo Boy (Figure 4-10, center). From this, it can be concluded that it seems to depend on formulation composition and type of nebulizer used if there are differences when nebulizing a stabilizer solution without or with nanocrystals. No differences in size distribution were obtained when nebulizing suspension B and pure solution with nebulizer Pari Turbo Boy (Figure 4-10, bottom). Although the influence of the formulation viscosity in the nebulization process has been previously reported in the literature (McCallion, Taylor et al. 1995), in this work it can be seen that viscosity values within the range of the references and nanosuspensions evaluated showed a negligible effect with the devices selected.

The LD diameters of the generated droplets were determined at the beginning of the nebulization process, in the middle (after 2.5 min) and at the end (5 min). Figure 4-11 shows the diameters obtained at these three time points, using the Multisonic nebulizer. The size distributions are again practically identical. That means with drug nanosuspensions a physically stable nebulized product with consistency in droplet size as a function of the time can be generated.

Detailed tables containing the LD diameters of aerosol droplets produced with jet and ultrasonic nebulization of BPQ nanosuspensions A and B, as well as for references solutions can be found in Appendix B.
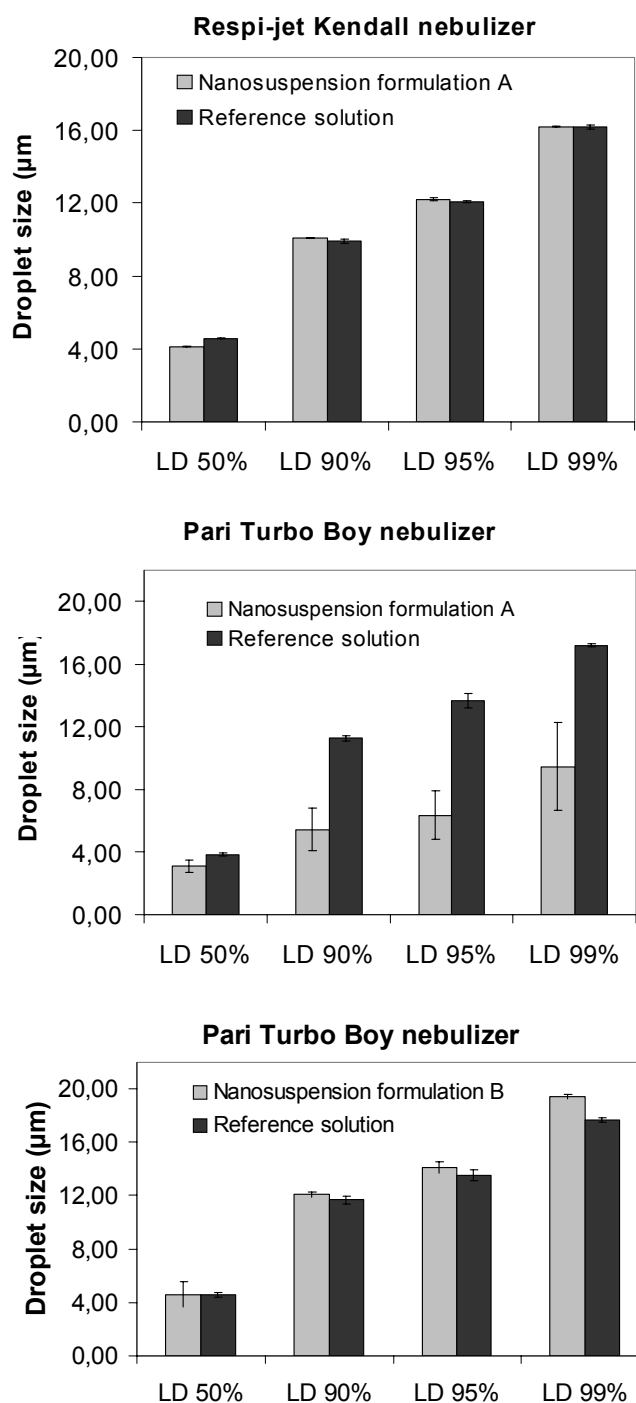
Figure 4-10: Size distribution obtained after nebulizing nanosuspension A using Respi-jet Kendall nebulizer and Pari Turbo Boy nebulizer (top and center) and nanosuspension B using Pari Turbo Boy nebulizer (bottom). All compared vs. the dispersion solution alone.
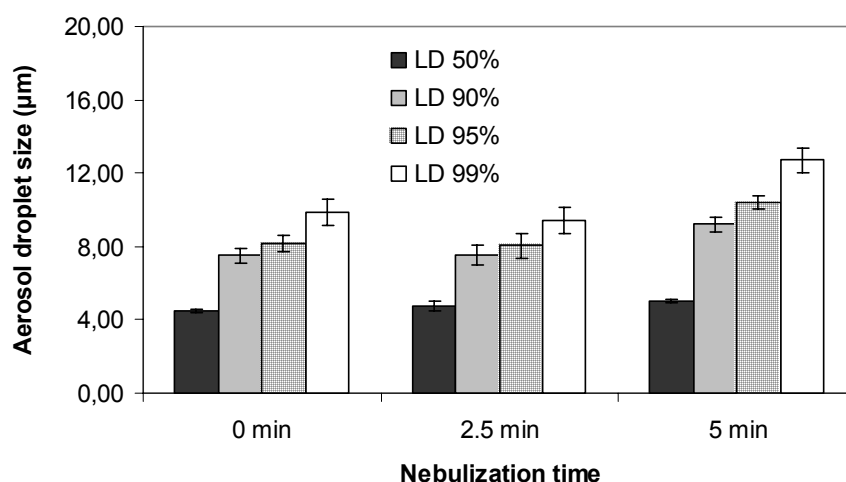
Figure 4-11: LD diameters characterizing the size distributions of nanosuspension formulation A nebulized with nebulizer Multisonic at the beginning (left), middle (center) and end (right) of the nebulization period, LD diameters d50%, d90%, d95% and d99%.

In the study it was found that formulation A could be nebulized very well with all the nebulizers used apart from Omron U1 that generated droplets of about 9-10 μm. Figure 4-12 shows the characterization parameters of the droplet size distribution obtained with the four different nebulizers when nebulizing nanosuspension A. As characterization parameters the LD diameters 50%, 90%, 95% and 99% were chosen. The diameter 100% is considered as less suitable because it is a problem of statistics if some very few large size droplets are detected. Typically the diameter d100% shows a higher variation whereas the d99% proves to be in all measurements rather consistent. Different nebulization technologies resulted in different size distribution for the same formulation, as expected from the specifications given by the manufacturer.

With both formulations, A and B, the dispersity of the particle size distribution (span) was smaller for the droplets produced with ultrasonic nebulizers than those produced with jet nebulizers with both formulations. Multisonic nebulizer showed a span value between 1.3 and 1.6 for both formulations, while the droplets produced by jet nebulizers showed values between 2.0 and 2.7.

The respirable percentage defined as the proportion of particles with appropriate size to reach the lung (percentage of particles < 5 μm), was a similar value for three of the nebulizers (~ between 50 and 60 %): Respi-jet Kendall, Pari Turbo Boy and Multisonic with both formulations tested. The percentage of particles under 5 μm

produced with Omron U1 nebulizer was considerable smaller than the one obtained with any of the other devices (~ 20 %), a situation already expected due to the d50% value measured with this device and by the reference values given by the manufacturer.
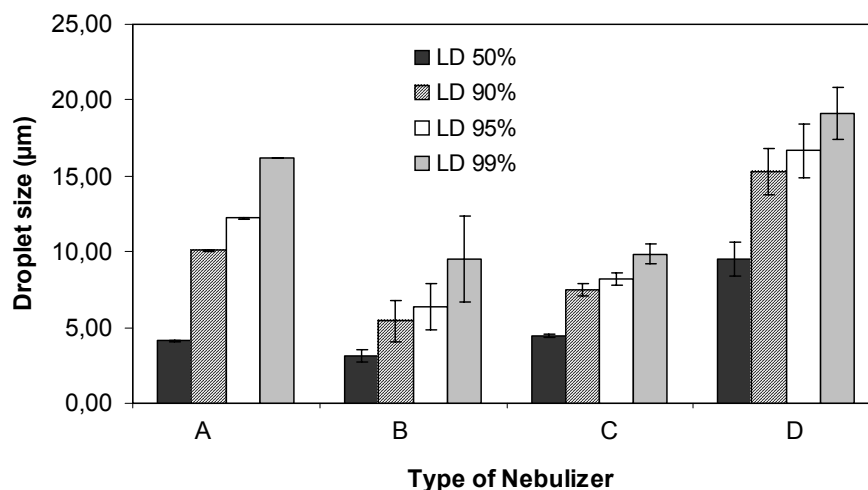

Figure 4-12: Characterization LD parameters diameters 50%, 90%, 95%, 99% of size distributions of nebulized suspension A with the nebulizers Respi-jet Kendall (A), Pari Turbo Boy (B), Multisonic (C), Omron U-1 (D). Sizes analysed at the beginning of the nebulization period.

However, there was also the effect that one nebulizer could very well nebulize suspension A and B whereas this was not the case with nebulizer Pari Turbo Boy. Figure 4-13 shows the aerosol size distribution obtained with two different suspension formulations but using the same nebulizer.

Of course it should be emphasised that from this one nanosuspension with less efficient nebulization it cannot be concluded that this nebulizer is less efficient. It is rather assumed that depending on the feature of each nebulizer system and the respective special properties of the nanosuspension formulation, one or the other nebulizer type may be optimal. The optimum system has to be established just by trial. The aerosol droplet diameter produced by jet nebulizers is directly proportional to the surface tension of the formulation (see section 2.5.1.3). The differences observed with nebulizer Pari Turbo Boy can be explained by the properties of both formulations. Formulation A has a slightly lower surface tension (39.6 mN/m) than

formulation B (44.1 mN/m), which influenced the formation of relatively larger droplets with the second formulation.
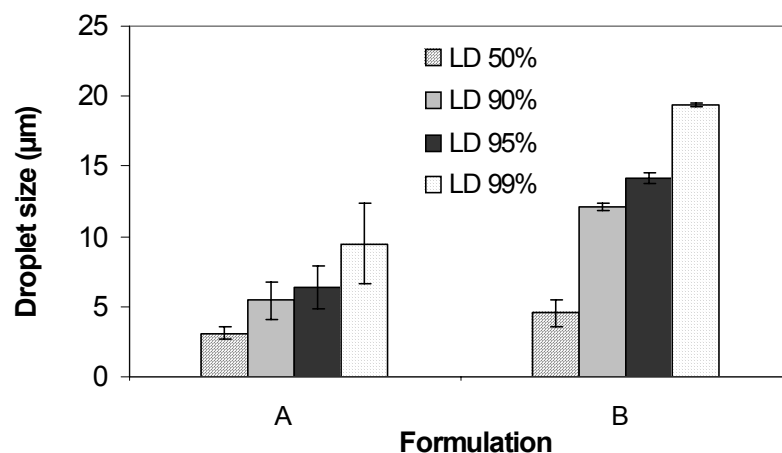

Figure 4-13: LD size distribution of drug nanosuspension A (left) and nanosuspension B (right) nebulized with nebulizer Pari Turbo Boy. Size distributions analysed at the beginning of the nebulization process.

It can be summarized that all the nebulizers investigated were able to efficiently nebulize drug nanosuspensions. Depending on the composition of the nanosuspension, the optimum nebulizer type may vary. For final judgement it would be necessary to nebulize a larger number of drug nanosuspensions being differently composed with regard to nanocrystal size, nanocrystal concentration and type and concentration of stabilizers. For reasons of practicability, it is recommended just to test different nebulizer types with the formulation in development.

4.1.2.2 Analysis of drug nanocrystals

For achieving a controlled delivery to the lungs it is a pre-requisite that no uncontrollable crystal aggregation occurs. Ideally crystal aggregation should be absent. Therefore to judge the performance of a nebulizer, apart from analysis of the droplet sizes it is also essential to analyse the crystal size in the droplets after nebulization. To do this, the aerosol stream was directed towards the wall of a glass beaker and the condensed aerosol droplets collected. The suspension was then analysed by laser diffractometry. Figure 4-14 shows the size distribution of the original drug nanosuspensions vs. the nebulized nanosuspensions.
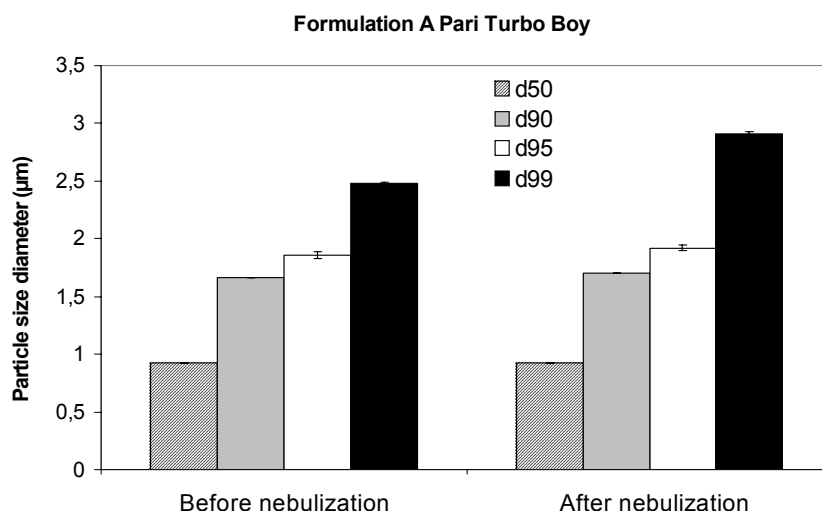
Figure 4-14: LD size distribution of the original drug nanosuspension (left) and drug nanosuspension A after the nebulization with the Pari Turbo Boy nebulizer, droplets were collected in the first half of the nebulization time (minute 0 – 2.5).

There is a minor shift to larger sizes (d99%) which from our point of view is not considered as impairing the *in vivo* performance, the diameters d50%, d90% and d95% were practically unchanged.

The drug nanosuspension does not only undergo a shear stress during nebulization, there is also an energy exposure in the reservoir of the nebulizer. Therefore it is also essential to analyse the nanocrystal size in the nebulizer reservoir. Figure 4-15 shows exemplarily size distribution of a nanosuspension stable in the reservoir and a suspension being less stable, both measured at the end of the nebulization process. The size diameters of the original nanocrystals is included here as reference. The diameter d99% increased from 2.5 to around 3.7 µm after nebulization. The d50%, d90% and d95% values remained within the same size as before nebulization.
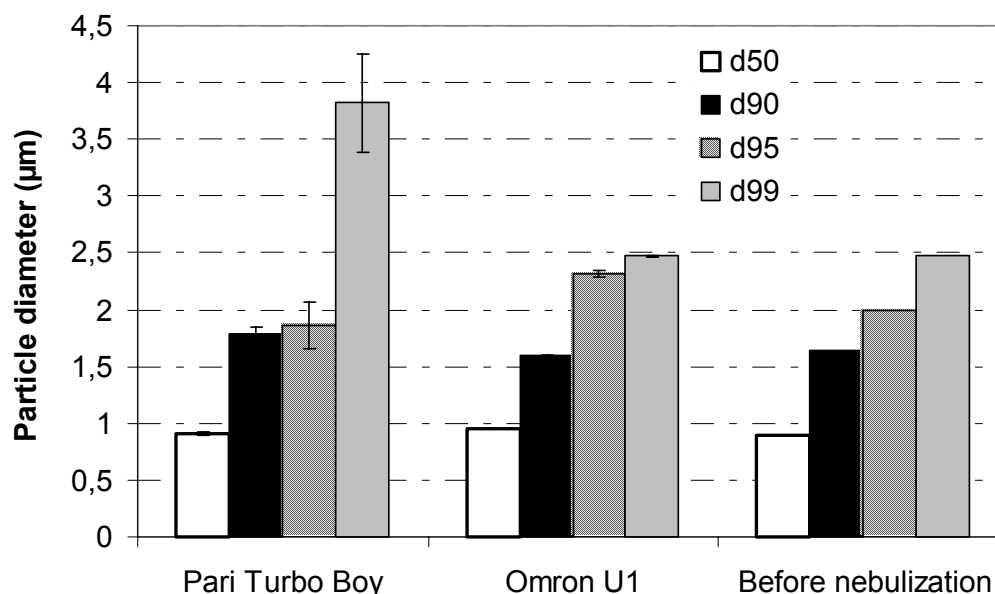
Figure 4-15: LD characterization parameters diameters d50%, d90%, d95% and d99% of suspension A in the reservoir of the nebulizer Pari Turbo Boy (left) and the nebulizer Omron U1 (right) at the end of the nebulization process compared to nanosuspension before nebulization (modified after (Hernández-Trejo, Kayser et al. 2005)).

Laser diffractometry is the most suitable method to detect crystal aggregates. As outlined above, the measurement range of PCS is approximately 3 nm – 3 µm. Particles slightly larger can be detected with a certain measuring error (sedimentation effect), but a few relatively large particles in the presence of a small-sized particle bulk population will not be detected anymore. The photon correlation signal "disappears" in the baseline of the correlation function. For highly sensitive analysis of size changes in the bulk population PCS was additionally applied. Figure 4-16 shows exemplarily the PCS diameters and polydispersity indexes of the drug nanosuspension before nebulization and after nebulization with the four nebulizer in the middle of the nebulization time.
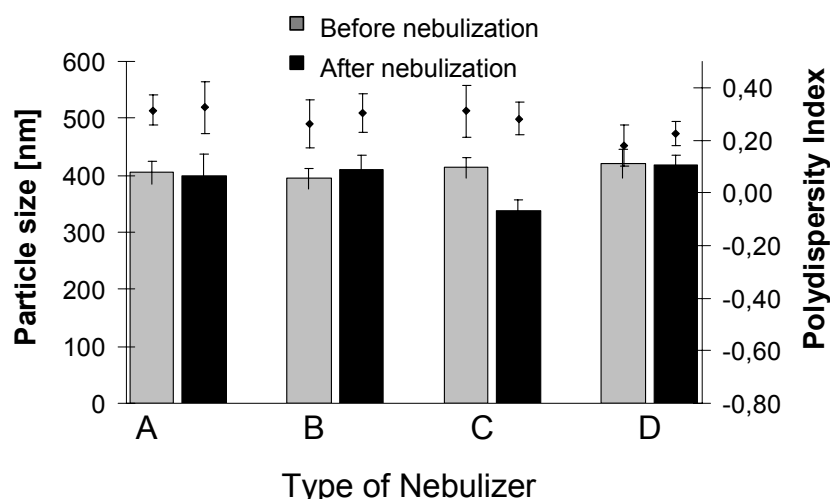
Figure 4-16: PCS diameters and polidispersity indexes of the drug nanosupension B (after (Hernández-Trejo, Kayser et al. 2005)) before and after its nebulization by Respi-jet Kendall nebulizer (A), Pari Turbo Boy nebulizer (B), Multisonic nebulizer (C) and Omron U-1 nebulizer (D).

In general there are slight but negligible increases in the PCS diameters and also the polydispersity indices indicating a certain change to the system. The data show nicely the sensitivity of the PCS being able to detect even relatively small differences. By this work it should be pointed out that the observed increases are not being considered as relevant for the *in vivo* performance. Especially it cannot be derived from the data that there are relevant performance differences of the nebulizers investigated.

In Figure 4-16 it can be noticed that the data obtained with the Multisonic nebulizer when nebulizing nanosuspension formulation B showed a diminution from about 400 nm to ~ 340 nm (see table 4-6 for initial data). This difference was attributed to the fundamental technology, which the Multisonic nebulizer uses for the generation of droplets. The standing waves produced on the surface of the nebulizer nanosuspension by the vibration of a piezolectric crystal let to the formation of water droplets. Therefore when a polydisperse nanosuspension is aerosolized, the smallest particles located on the surface of the sample will therefore be preferentially loaded into the droplets formed.

PCS analysis was also employed to monitor the change in crystal size in the reservoir as a function of nebulization time. Figure 4-17 shows exemplarily the

change in PCS size and PI as a function of time for two nebulizers. There is a slight increase easily detectable by PCS.
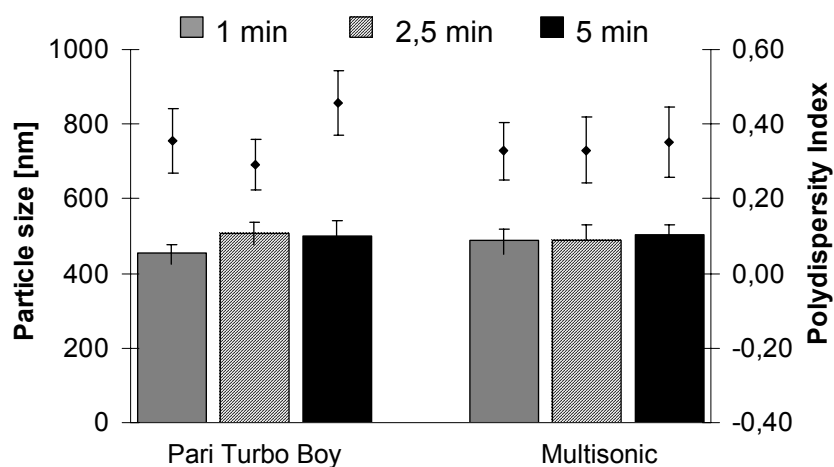

Figure 4-17: PCS diameters and polidispersity indexes (PI) of nanosuspension A as a function of nebulization time (1 min, 2,5 min, 5 min), Pari Turbo Boy nebulizer (left) and Multisonic nebulizer (right).

4.1.3 Drug output from jet nebulizers

Basic advantage of drug nanocrystal suspensions compared to suspensions of micronized drugs is that the crystals are more evenly distributed in the aerosol droplets. In case of drug microcrystals, very often the number of aerosol droplets is higher than the number of drug microcrystals. In such a case, a fraction of the aerosol droplets will contain no drug crystals at all, many droplets will contain one crystal and a certain fraction more than one crystal. Transfer of drug microcrystals to nanocrystals increases the number of drug particles, that means the likelihood of having crystals in each droplet increases. As a result one has a more even distribution of crystals to all droplets (to be more precise: same concentration of crystals per volume unit droplet). This is schematically shown in Figure 4-18.
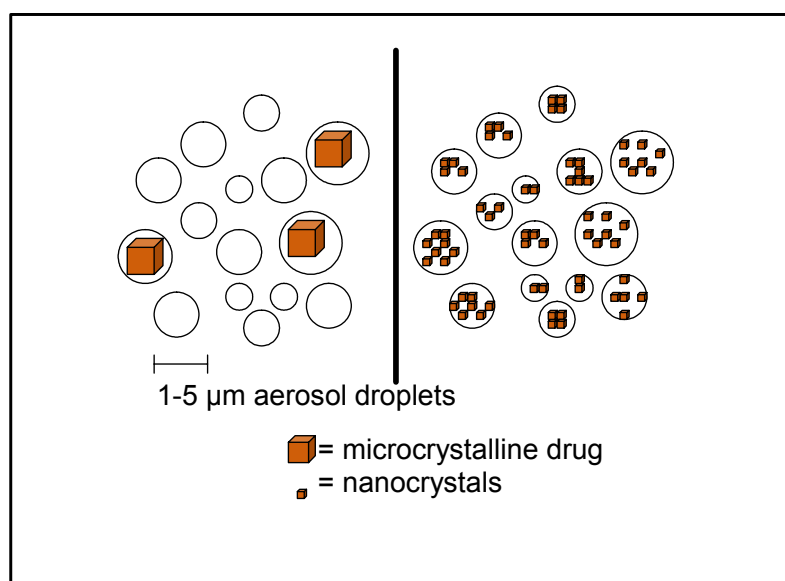
Figure 4-18: Graphic representation of the distribution of microcrystals (left) and of nanocrystals (right) in aerosol droplets. (Modified after (Jacobs and Müller 2002)).

4.1.3.1 Theoretical calculation of the nanocrystals load per aerosol droplet

The theoretical increase of drug nanocrystals loading per droplet, can be calculated assuming spherical droplets. The size of the droplets produced by the nebulization system should be included in the formula (Ostrander, Bosch et al. 1999):

$$\text{Volume of a spherical particle} = \frac{4}{3}\pi\,r^3$$

where r represents the droplet radius.

Only for theoretical calculation purposes, the example of the nebulization system Pari LC Star attached to a Pari Boy air compressor is considered in the following paragraphs. The average diameter of the droplets (50 % of the droplets under that diameter) specified by the manufacturer is 2.8 µm using saline solution. Another basic information, assumed here is that the average diameter of the buparvaquone nanocrystals obtained is typically around 400 nm with cubic shape. The calculations in order to determine the "maximum" crystal load of 2.8 µm droplets are shown in Table 4-7:

Table 4-7: Theoretical calculations to determine the maximum BPQ nanocrystals (400 nm) load in 2.8 μm aqueous droplets. The maximum of microcrystals (2 μm) load in the same size droplets are calculated for comparison

PARAMETER	FORMULA	RESULTS
Volume of 2.8 μm droplets	$= \dfrac{4}{3}\pi(1.4\text{x}10^{-6})^3\,m^3$	$= \dfrac{4}{3}\pi(2.74\text{x}10^{-18})m^3$
Volume of 400 nm crystals	$= (4\text{x}10^{-7})^3\,m^3$	$= (6.4\text{x}10^{-20})m^3$
# of 400 nm crystals per 2.8 μm droplet	$= \dfrac{\text{Volume of 2.8 }\mu\text{m droplet}}{\text{Volume of 400 nm drug crystal}}$	$= \dfrac{\dfrac{4}{3}\pi(2.74\text{x}10^{-18})}{(6.4\text{x}10^{-20})} = 179$
Volume of 2 μm crystals	$= (2\text{x}10^{-6})^3\,m^3$	$= (8\text{x}10^{-18})m^3$
# of 2 μm crystals per 2.8 μm droplet	$= \dfrac{\text{Volume of 2.8 }\mu\text{m droplet}}{\text{Volume of 400 nm drug crystal}}$	$= \dfrac{\dfrac{4}{3}\pi(2.74\text{x}10^{-18})}{(8\text{x}10^{-18})} = 1.4$

Theoretically it is possible to include as many as 179 crystals of 400 nm in each 2.8 μm droplet, "assuming cubic crystals", while only 14 crystals of 2 μm can be present in each 10 droplets of the described size.

In order to include in the calculation the effect of the drug concentration in the formulation, it is important to calculate the volume of drug per mL of formulation and the number of crystals in that volume. Details of these calculations are given in Table 4-8, assuming a 5% of drug in the nanosuspension (density 1 g/cm^3).

Table 4-8: Theoretical calculations to determine the nanocrystals load in aerosol droplets produced with a 5% nanosuspension

PARAMETER	FORMULA	RESULTS
Volume of drug in 1 mL	5% w/w drug = 0.050 mL	= 0.050 cm^3
Volume of vehicle in 1 mL	95 % w/w vehicle = 0.95 mL	= 0.95 cm^3
# of 400 nm crystals occupying 0.050 cm^3	$= \dfrac{\text{Total volume of drug in 1mL}}{\text{volume of drug crystal}}$	$= \dfrac{0.050 \text{cm}^3}{(6.4 \times 10^{-14})\text{cm}^3}$ = 7.81 x 10^{11} crystals
# of 2.8 µm droplets occupying 0.95 cm^3	$= \dfrac{\text{Total volume of vehicle in 1mL}}{\text{volume of 2.8 } \mu\text{m droplet}}$	$= \dfrac{0.95 \text{ cm}^3}{\frac{4}{3}\pi(2.74 \times 10)^{-12} \text{ cm}^3}$ = 8.28 x 10^{10} droplets
# of 400 nm crystals per 2.8 µm droplets of vehicle	$= \dfrac{\text{number of 400 nm crystals}}{\text{number of 2.8 } \mu\text{m droplets}}$	$= \dfrac{7.81 \times 10^{11} \text{ crystals}}{8.28 \times 10^{10} \text{ droplets}}$ **= 9 nanocrystals**
# of 2 µm crystals occupying 0.050 cm^3	$= \dfrac{\text{Total volume of drug in 1mL}}{\text{volume of drug crystal}}$	$= \dfrac{0.050 \text{cm}^3}{(8 \times 10^{-12})\text{cm}^3}$ = 6.25 x 10^9 crystals
# of 2 µm crystals per 2.8 µm droplets of vehicle	$= \dfrac{\text{number of 400 nm crystals}}{\text{number of 2.8 } \mu\text{m droplets}}$	$= \dfrac{6.25 \times 10^9 \text{ crystals}}{8.28 \times 10^{10} \text{ droplets}}$ = 0.075 microcrystals

That means, a maximum of ~ 9 drug nanocrystals will be contained per each droplet (2.8 µm) produced, considering a very homogeneous suspension. Approximately 75 microcrystals can be incorporated in each 1000 droplets of 2.8 µm with the concentration calculated. From these calculations, it can be seen that the number of crystals per droplet, is logically expected to be directly proportional to the concentration of drug nanocrystals in the formulation. An increase in the concentration of BPQ nanosuspension nebulized can reduce the nebulization volume and nebulization time required to achieve the effective dose in the lung. However, the concept of increasing the drug concentration in the formulations, needs to be considered carefully. Highly viscous formulations can reduce the efficiency of the nebulization process as it will be discussed in the following sections.

4.1.3.2 The effect of the physicochemical properties of the dispersion media on the droplet size distribution of jet nebulizers

Although the increment of the drug concentration in the nanosuspension ensures the higher drug loading of the droplets, further formulation considerations need to be analyzed before deciding the optimal nebulization formulation. The increase of the percentage of drug may lead to an increase in the formulation's viscosity and consequently reduce the efficiency of the nebulization process. Furthermore, in the case of jet nebulizers, the nebulization rate is inversely proportional to the surface tension and the viscosity, as it has been explained in section 2.5.1.3.

Due to this fact, in a second study the influence of the increment of the drug nanocrystals concentration on the performance of the nebulization process was investigated (Hernández-Trejo, de Boer et al. 2005). In order to evaluate the nebulization performance of the formulations, the following parameters were evaluated:

➢ Mass median diameter (MMD) of the droplets produced

➢ Span, as a measure of the dispersion of the droplet size distribution

➢ Percentage of dose emitted

➢ Nebulization time

➢ Percentage of droplets < 3 µm

The percentage < 3 µm is considered of interest in this work, as the target area of deposition of buparvaquone nanocrystals is the deep alveoli, which requires particles smaller than 3 µm. In this study, the jet nebulizer Pari LC Star, developed for the delivery drugs in the alveolar area of the lung, was used attached to a Pari Boy compressor (Pari GmbH). The reason for that is that this jet nebulizer is one of the few devices actually in the market capable to deliver a very fine aerosol distribution, ensuring the delivery of a MMD appropriate for peripheral deposition in the lung, where *Pneumocystis* infection is localized.

For this set of experiments, the formulations composition of the nanosuspensions used are given in Table 4-9.

Table 4-9: Composition of buparvaquone nanosuspensions used with Pari LC Star jet nebulizer

EXCIPIENTS	% w/w aqueous formulations				
	C	D	E	F	G
Buparvaquone	1.0	1.0	1.0	2.0	7.0
Polox. 188	0.5	-	0.5	0.5	0.5
Phospholipon 80	0.5	-	-	-	-
Sodium glycocholate	0.3	-	-	-	-
Tyloxapol	-	0.3	0.15	0.15	0.15
Glycerol 85%	2.5	2.5	2.5	2.5	2.5

Formulations were nebulized under the same conditions (see section 3.2.3). A summary of the results obtained with this nebulization tests is given in Table 4-10. The MMD of droplets produced nebulizing *water*, using the system described, was 2.87 µm, with a percentage of particles < 3 µm of 54.6%. A reduction of the droplet size was observed when nebulizing the nanosuspensions formulated. When nebulizing our nanosuspensions (fill volumes of 5 mL), the diameter of the droplets produced with nanosuspensions were within the range from 1.72 to 1.99 µm depending on the formulation composition. A very small increase from 1.72 to 1.87 µm was observed when the drug concentration was increased from 1 to 7% in the formulation.

In all cases, the formulation was nebulized until the sputtering and the drug residues in the nebulizer reservoir were analyzed with a UV spectroscopy method. In all the cases, the nebulization time was around 7 min, meaning that it was perfectly possible to deliver within less than 10 min (sputtering times ~ 7 min), doses of approximately 40 mg, 80 mg and 197 mg contained in water droplets of appropriate size to reach the deep area of the lung (in all cases ~ 2 µm).

Table 4-10 Aerosolization characteristics of different nanosuspension formulations following nebulization with Pari LC Star nebulizer. A fill volume of 5 mL was used in all the cases.

Parameter	Buparvaquone formulations				
	C	D	E	F	G
Nebulization time until sputtering (min)	7'30"	7'10"	7'30"	7'30"	7'30"
Mean drug output (mg) at 40 L/min (inhalation)	46.67	63.12	52.64	117.56	297.59
Mean residue in the reservoir (mg)	15.73	9.98	10.96	25.99	72.71
Mean % of drug emitted	**74.79**	**86.35**	**82.77**	**81.89**	**80.36**
Mass Median Diameter (MMD) (µm)	1.96	1.99	1.72	1.78	1.87
Span	1.85	1.75	1.78	1.81	1.76
% < 3 µm (respirable dose)	**75.38**	**75.70**	**82.18**	**80.32**	**78.80**
Mean surface tension (mN/m)	28.23	27.67	30.15	33.73	33.33
Mean viscosity (mPa*s)	1.074	1.010	1.015	1.040	1.083
Mean osmolarity (mOsmol/kg)	267.3	258.0	252.7	235.0	222.0
Mean density (g/cm^3)	1.007	1.005	1.005	1.006	1.008
pH	6.00	6.70	6.11	6.20	6.43

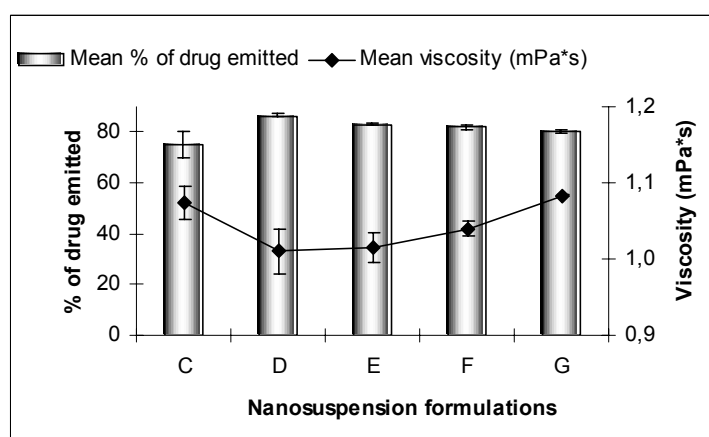* Nebulizer experiments were performed in duplicate

The percentages of drug output obtained for the 1, 2 and 7% nanosuspensions (E, F and G) were 83, 82 and 80 % respectively. The percentage of the droplets < 3 μm was in each case, 82.2, 80.3 and 78.8 % accordingly. The high drug output obtained with the nanosuspension formulations seems to be highly favoured by the reduction of the surface tension due to the presence of surfactants in the vehicle.

With these experiments, it was confirmed that there is no diminution of the nebulization efficiency when increasing the concentration from 1% to 7% of drug. The viscosity of the nanosuspension increased only from 1.02 to 1.08 mPas*sec, while the surface tension remained approximately constant, as the quantities of surfactants in the formulation did not differ.
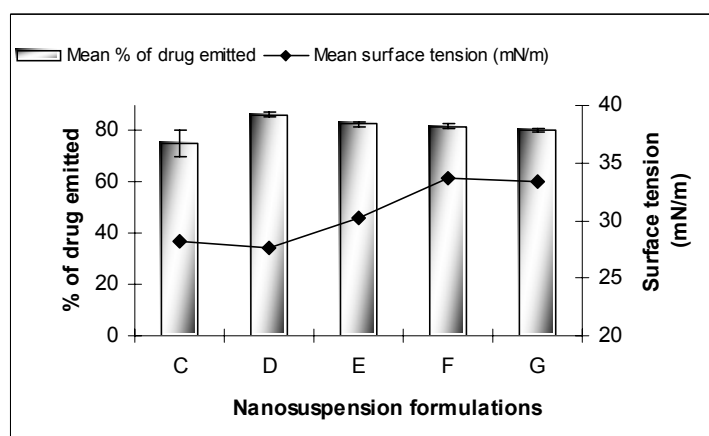
The Figure 4-19 represents the influence of the viscosity (a) and surface tension (b) of the nanosuspension formulation on the percentage of drug output from the Pari LC Star nebulizer. As expected for jet nebulizers, lower surface tension and viscosity values resulted in an improvement in the quantity of drug emitted by the nebulizer.

Although the in vitro characterization of the aerosol produced by the nebulizer Pari LC Star has shown promising results, it is important to remember that the real percentage of these doses reaching the deep lungs will of course depend on the breathing profile of each patient as well as the morphological and physiological condition of the lung in disease.

Nevertheless, the delivery of high doses can be considered an advantage of this delivery system in cases when such quantities of the drug are necessary to reach the therapeutic effect. Nebulization of drug nanocrystals may offer a big advantage to deliver the desired quantity of drug at once, within acceptable nebulization times, ensuring patient acceptance.

(a)

(b)

Figure 4-19: Percentages of drug emitted obtained with different nanosuspension formulations using a Pari LC Star nebulizer. (a) Represents the influence of viscosity and (b) the influence of the surface tension values on the quantity of drug emitted.

4.1.3.3 Drug nanocrystals aggregation with Pari LC Star nebulizer

The determination of potential aggregation of the drug nanocrystals using the Pari LC Star nebulizer was investigated for formulations C-G. The nebulizer was operated for 5 minutes, and samples were collected from the nebulizer reservoir before and after nebulization. Additionally, the aerosol was collected during the 5 minutes nebulization process using the method described in section 3.2.3.3. Drug nanocrystals were measured with PCS and LD techniques. The summarized particle diameter obtained is shown in Figure 4-20. In general, there was no effect of the nebulization process on the nanocrystals particle size.
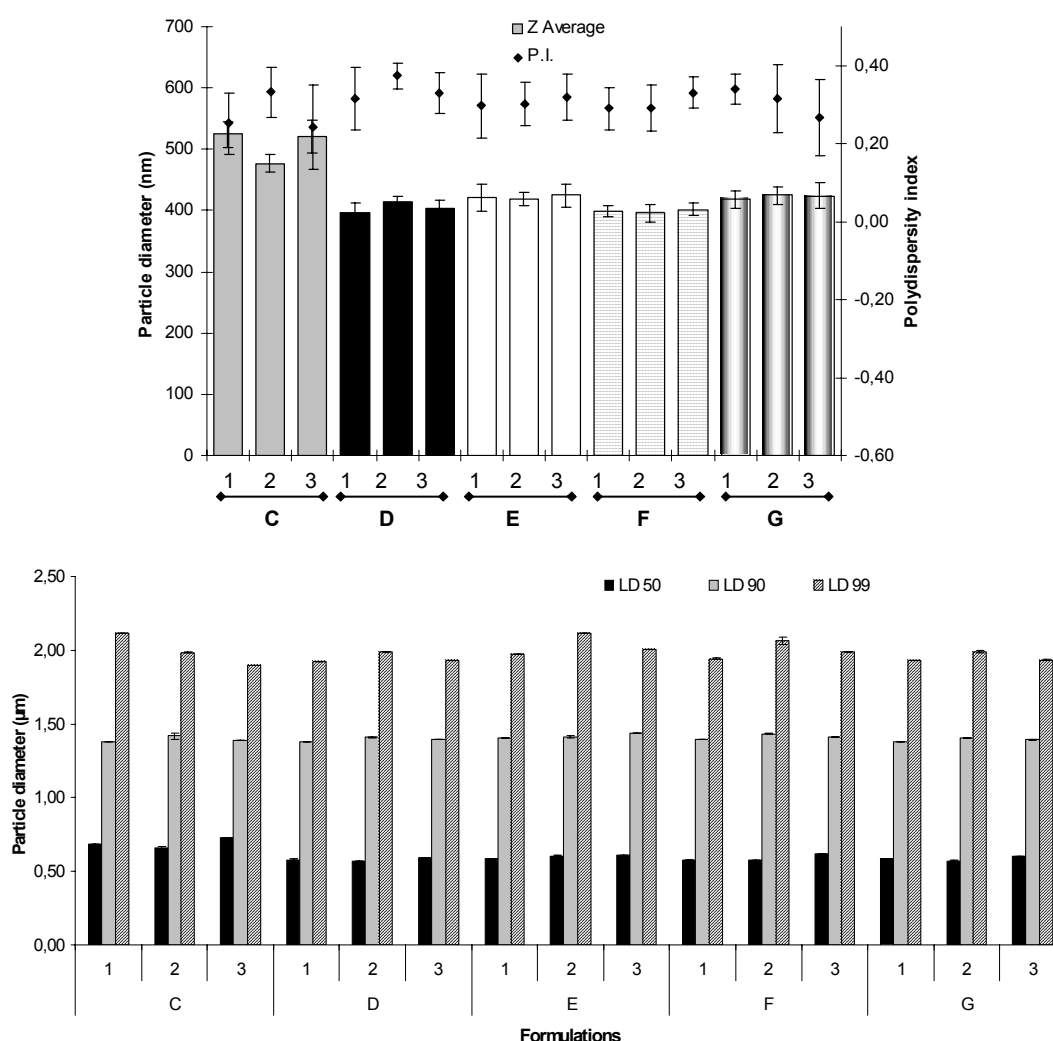

Figure 4-20: Influence of the nebulization process on particle size diameter using Pari LC Star and formulations C-D. PCS and LD particle diameter are shown at the beginning (1), at the end (3) of the nebulization and the diameter of particles detected in the aerosol collected (2).

4.1.4 Conclusions

This part of the thesis shows that the drug buparvaquone can be successfully formulated as nanosuspension by high pressure homogenization, yielding drug nanocrystals with acceptable diameter to be incorporated into water aerosol droplets and – from the measured droplet size –can reach the site of action in the lungs. It was shown that with both nebulization technologies, jet or ultrasonic, the composition of the formulation will influence the aerosol droplet size produced. It can be conclude that the best formulation-nebulization system combination can only be found by trial. Regarding the aggregation of the nanocrystals influenced by the nebulizer technology, it could be seen that it can be optimized by the formulation composition.

Pneumocystis pneumonia therapy or prophylaxis via inhalation requires penetration of the drug to the peripheral lung region and the appropriate droplet size distribution of the aerosol to be inhaled will be determinant for their deposition. The aerosolization several formulations produced droplets in the range 1.7-2 μm, an appropriate value to predict central and pheripheral deposition, using the Pari LC Star nebulizer attached to a Pari Boy compressor. The size distribution of the aerosol is favoured by the presence of surfactants in the formulation.

It was demonstrated that the increment on drug content in the nanosuspensions from 1% to 7% did not decrease the efficiency of the nebulizer, evaluated as the percentage of dose emitted and % of aerosol droplets < 3 µm. The physicochemical characteristics of the formulation, specially the surface tension will affect directly the percentage of dose emitted. Surfactants yielding the lowest surface tension values consequently emitted the highest quantity of drug i.e. had the lowest residual volumes. These experiments have demonstrated the efficiency of nanosuspensions to deliver higher doses of antimicrobial in relatively short administration time (all cases ~7min).

4.2 Inhalation of buparvaquone nanocrystals in the therapy of *pneumocystis* pneumonia infected mice

4.2.1 Physical and microbiological characterization of the buparvaquone nanosuspension

Photon correlation microscopy revealed an average drug nanocrystals size of 418 ± 22 nm with a polydispersity index of 0.32 ± 0.05. The formulation was also investigated for the presence of microparticles by means of a laser diffractometer. The percentages of nanocrystals found to be smaller than a certain diameter were d50% <0.5 ± 0.01 µm, d90% < 1.3 ± 0.01 µm and d99% <2.2 ± 0.12 µm. The average diameter of the drug nanocrystals indicated a satisfactory reduction (~ 400 fold) in the size of the original crystalline material (Hernández-Trejo, Kayser et al. 2005). The fact that the drug nanocrystals were smaller than the average size of the aerosol droplets (see below) was also an important parameter for the quality acceptance of the formulation.

The response to drug particles administered by inhalation in a disease such as PcP, is related not only to the amount of drug particles deposited in the alveoli, but also to the length of time these particles are retained in the lung and whether they are dissolved before being cleared. Due to its amphiphilic property, soy phosphatidylcholine was chosen to stabilize this dispersion of a lipophilic drug crystals in aqueous media. While the charged side of the molecule makes it hydrophilic, the uncharged opposite end facilitates the wetting effect of the phospholipids on the surface of the lipophilic buparvaquone crystals (favored by the high pressure homogenisation process). Another reason for choosing this surfactant was that phospholipids are the primary natural component of cell membranes and thus of the surfaces available for absorption in the lung. Natural lung surfactants consists by 80-90% of lipids, of which phosphatidylcholine makes 70 to 80% (McAllister, Alpar et al. 1996). Pulmonary surfactant promotes the displacement of particles from air to the aqueous phase and that the extent of particle immersion depends on the surface tension of the surface active film. The lower the surface tension, the greater is the immersion of the particles into the aqueous subphase. Phospholipidic interactions between natural surfactants and the phospholipids on the surface of BPQ nanocrystals were expected to enhance the dissolution of the drug

nanoparticles in the lung at the air-liquid and liquid-solid interfaces. These interactions may also favor penetration of the respiratory epithelium rather than rapid particle clearance.

Finally, the absence of microbiological contamination in the formulation supports its suitability for pulmonary administration. Standard microbiological tests were applied to the formulation. The suspension was inoculated on sheep blood, Mueller-Hinton and Emmons' neutral Sabouraud's dextrose (NSDA) agar plates for the investigation of pathogenic bacteria, general microorganisms and fungi respectively. Samples were controlled after 48 and 72 h incubation at 25 and 37 °C under 5% CO_2 and humidity saturated atmosphere. Samples showed sterility under the conditions tested.

4.2.2 Particle size distribution of the atovaquone suspension

The size distribution of the microcrystals contained in the product Wellvone$^{®}$ was characterized using LD technique. As the concentration of the suspension is 150 mg/mL, a dilution was done in order to obtain a more suitable volume to deliver per animal. 1 mL of the original suspension was diluted to a volume of 15 mL using a 2.5% glycerol solution. Original and diluted microsuspension were measured to discard particle size disruption due to the dilution process. The Table 4-11 summarizes the size distribution obtained for both products.

Table 4-11: Particle size distribution of Wellvone$^{®}$ as supplied and after dilution. Measurements were performed with a laser diffractometer. Data was obtained using the Mie theory (refraction index real = 1.456, imaginary = 0.01). Sample was diluted in water.

Volume size diameter (µm)	Wellvone$^{®}$	Wellvone$^{®}$ diluted
d50%	0.93 ± 0.01	1.01 ± 0.01
d90%	3.16 ± 0.01	3.20 ± 0.02
d95%	4.13 ± 0.02	4.18 ± 0.03
d99%	5.48 ± 0.01	5.51 ± 0.01

4.2.3 Characterization of the aerosol distribution and nebulizer performance.

The uniformity of the aerosol distribution was determined using an aerosol cascade impactor (ACI) and following standard procedures. The MMAD is defined as the diameter at which half of the total aerosol mass is contained in larger particles and half in smaller ones. The MMAD of the aerosol droplets produced by the nebulizer was 2.65 ± 0.06 μm (n = 3 measurements). The average percentage of particles < 3.3 μm was 67%, while 96% of the particles where < 4.7 μm, and 5% < 1.1 μm. The resulting geometric standard deviation (GSD value) was 1.68, implying that this aerosol (as most therapeutical aerosols) was polydisperse. It is generally understood that aerosols with a GSD <1.22 are monodisperse (Fuchs and Sutugin 1966). The GSD value obtained for the aerosol cloud produced by this nebulizer was considered normal and satisfactory considering the compressed gas flow rate used for the operation of the nebulizer.

The efficiency of a nebulization device is described not only by the size distribution of the droplets it produces, but also by the relative amount of drug emitted compared to that retained in the reservoir. When nebulizing a fill volume of ~6 ml buparvaquone nanosuspension, our device emitted 69.6 ± 1.2% (n = 6 measurements) of the original dose. The performance of the nebulizer was considered appropriate to nebulize the 1% BPQ formulation used here.

4.2.4 Drug distribution after specified inhalation exposure times

Although we were able to estimate a theoretical dose available for inhalation by the animals by using the calculus already described (see section 3.2.4.3), the actual uptake by the mice depends on a multitude of ponderable, e.g. breathing pattern, shape of the particles, length of exposition of the animals to the aerosol, and imponderable entities. It is widely accepted that in humans, aerosol particles with an aerodynamic diameter of < 3 μm tend to penetrate deeper into the lungs (Gonda 1988). Previous investigations on aerosol deposition in small laboratory animals (Raabe, Al-Bayati et al. 1988) showed that in mice, only 1% of the given dose will be deposited in the lung when inhaling aerosols of about 3.45 μm in diameter. However, these studies may not be fully comparable to the present study, mainly due to differences in inhalation methodology (multiport head-only exposure apparatus versus the inhalation chamber used here).

Therefore, in a preliminary experiment we investigated the quantities of drug deposited in WT (wild type) mice by our inhalation exposure system. A summary of the distribution of the drug in selected organs after varying duration of exposure to the aerosol is given in Figure 4-21.
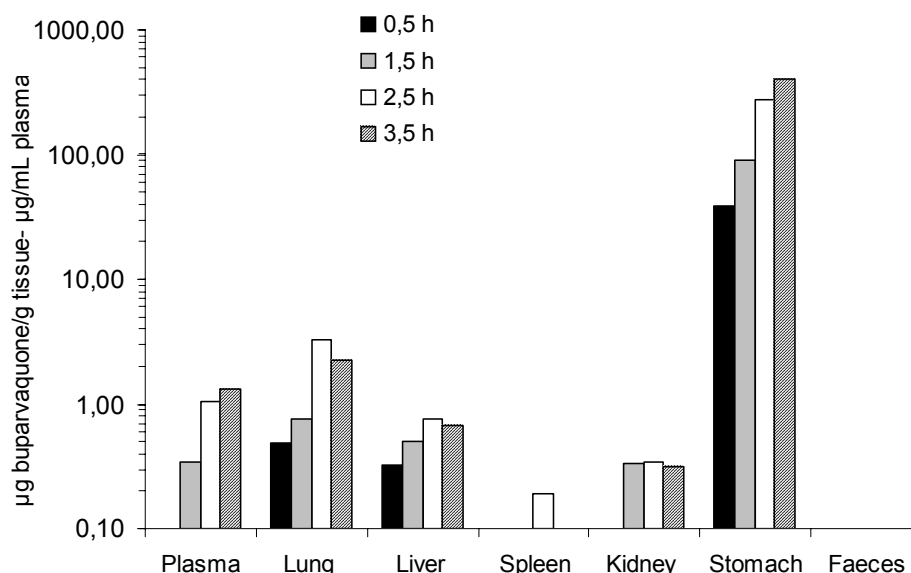

Figure 4-21: Distribution of aerosolized buparvaquone in different mouse tissues. One mouse per exposure time. A second experiment following identical procedures gave essentially the same results (data not shown). Plasma values in µg drug per ml plasma.

The quantities of BPQ detected in the lungs of these mice were 0.49-0.58 µg/g tissue for those animals exposed for half an hour and increased to values ranging 0.76-0.68 µg/g, 3.29-2.65 µg/g, and 2.2-1.62 µg/g for mice 1-mice 2 exposed to 1.5 h, 2.5 h, and 3.5 h, respectively. We were able to detect a non-linear but defined improvement in lung deposition up to 2.5 hours of exposure. After that, a maximum number of retained particles seemed to be reached, suggesting an equilibrium with the rate of particle clearance. This trend, however, was not observed in plasma, where values constantly and reproducibly increased from 0.00-0.00 µg/ml to 1.06-1.15 µg/ml, and 1.32-2.95 µg/ml after single exposure for 0.5 h, 2.5 h, and 3.5 h, respectively. The highest amount of BPQ, however, was found in the stomach (Figure 4-21). This might be explained by the different mechanisms of particle clearance, depending on their site of deposition. In general, as long as the particles are not dissolved, there are two major clearance pathways for particles administered as aerosols: removal

from the lung by the mucociliary "escalator" and phagocytosis by the alveolar macrophages (Gronenberg, Witt et al. 2003). When particles are deposited in the ciliated airways, they will be cleared primarily by mucociliary movements. The ciliated epithelial cells of the airways and nasal passages are covered with mucous which they keep in constant flow towards the pharynx, where it mixes with saliva and is swallowed down into the gastrointestinal tract. The speed and rate of particles and (dead) cells cleared from trachea and small airways is faster than the clearance of particles in nonciliated compartments such as the alveoli. It is assumed here, that the relatively large quantities of BPQ detected in the stomach result from the mucociliary clearance of aspirated material rather than from oral uptake of material deposited on the fur or the chamber wall, especially as we did not observe any pronounced preening or licking the chamber wall during or after exposure to the aerosol.

The quantities of drug found in the liver and kidneys are indicative of a rapid transport of the administered drug nanocrystals. The predominant and constant values observed in the liver, might also point to an enterohepatic recirculation of the drug as has been reported for the 1,4-naphthoquinone atovaquone (GlaxoSmithKline 2001).

4.2.5 Responses to treatment of *Pneumocystis* pneumonia among groups

The assessment of the *P. murina* burden in lung homogenates was based on the $\log_{10}$ nuclei numbers/lung as counted in BB-stained microscopical preparations. Figure 4-22 compares the data obtained for the individual groups. Data from treated and non-treated control groups were tested for normality using the Shapiro-Wilk test. The result showed no significant evidence of deviation from normality in all five experimental groups (95% confidence level). The Bartlett's test for equality of variances indicated that variances were not significantly different (P = 0.49). Based on these results, the analysis of variance (one-way ANOVA) with Turkey's Post-Hoc test was used to analyze differences and allow multiple comparisons between the groups (95% confidence level).
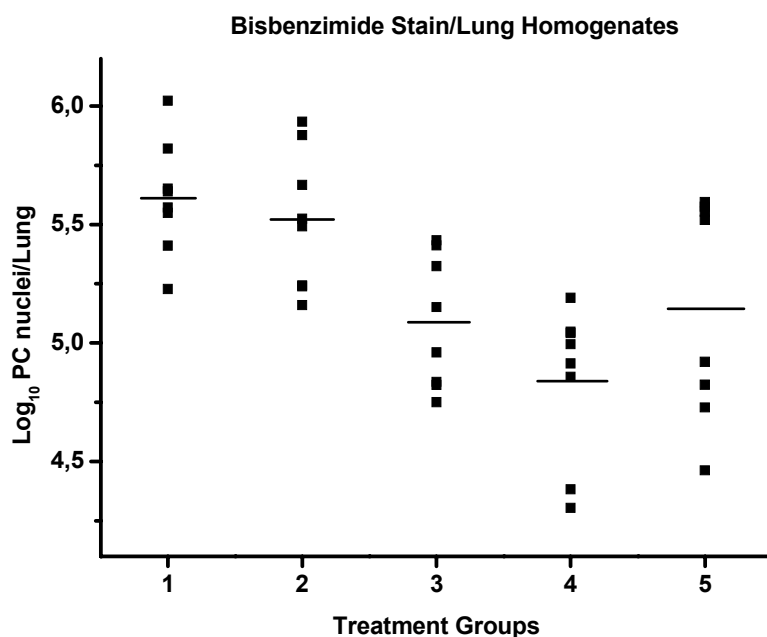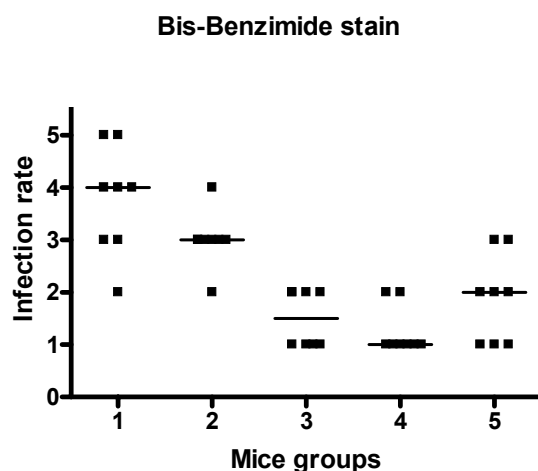
Figure 4-22: ***Pneumocystis* burden as microscopically determined in lung homogenate preparations using the bisBenzimide stain.** Groups of 8 *P. murina*-infected RAG mice were treated as follows for 3 weeks (5 days a week) before sacrifice: 1 = untreated, 2 = 30 min exposure to aerosolized placebo dispersion, 3 = 20 mg BPQ nanosuspension/ kg mouse per os, 4 = 30 min exposure to aerosolized BPQ nanosuspension, 5 = 20 mg ATQ suspension/ kg mouse per os
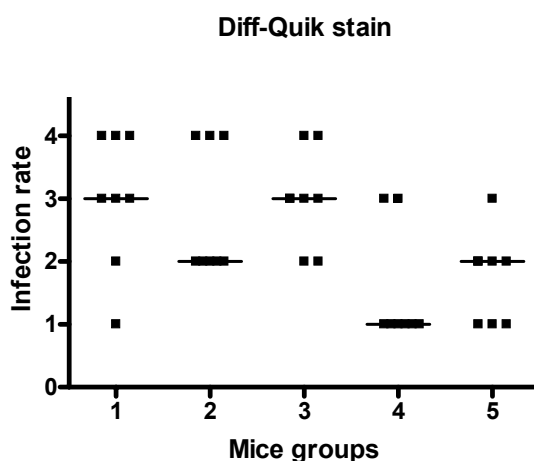
The analysis of variance (F statistic used) showed a significant difference between the groups and within the groups (P = 0.0002). Paired multicomparisons showed no significant difference between the negative control group and the group receiving the placebo aerosol formulation (P = 0.978). Both groups that had received the BPQ nanosuspension, either as an aerosol or per os, showed a significant reduction of pathogens burden when compared with the negative control group. The significant P values obtained were 0.0004 and 0.023 for aerosol and for the oral administration, respectively. The comparison between the placebo group and the group that had received BPQ as aerosol also showed the expected significant reduction of infection (P = 0.002). The difference in microorganisms load between the group that had received BPQ as aerosol and the one that had received PBQ per os, however, was

statically not significant (P = 0.576). Finally, the pathogen burdens of the negative control group did not differ significantly from that of the group that had received the ATQ formulation per os (P = 0.056) despite the fact that oral ATQ is recommended for treating moderate PcP. The reason for that cannot be convincingly concluded from these experiments. As some reduction in microorganism burden could be observed, it seems as if the duration of ATQ therapy (15 days in total) might not have been long enough to significantly improve the infection status of this group. The difference between the groups receiving oral administration of BPQ and ATQ was also statistically not significant (P = 0.996) even though observations in individual mice suggested differently. These inconclusive results may be attributed to the high variation between the 8 animals of the group having received ATQ per os (see Figure 4-22).

A somewhat different evaluation of the infection burden was based on the quantification of parasites in BB-stained (Figure 4-23a) or DQ-stained (Figure 4-23b) lung impression smears (for details, see section 3.2.4.9). The numbers of pathogens per lung impression smear were summarized as an arbitrarily defined infection score (0 to 5) per animal. The scores obtained with the BB-stain for the five experimental groups are shown in Figure 4-23a. The statistical comparison of these groups of data was performed using the Kruskal-Wallis analysis of variance by ranks followed by the Dunn's Post-Hoc test to allow multicomparisons (Zar 1984). The P values calculated with these groups of data showed a very similar tendency as that data obtained from analyzing the lung homogenates. The difference between and within groups calculated with the Kruskal-Wallis analysis were significant (P = 0.00003). Multicomparisons showed a significant difference between the negative control group and those groups that had received BPQ per os, aerosolized BPQ, or ATQ per os (P <0.01, <0.001, and <0.05, respectively). Again a significant difference in *P. murina* burdens was observed between the groups that had received aerosolized placebo versus the BPQ formulation (P <0.01). No significant difference resulted from the comparison between the groups that had received oral versus aerosolized BPQ, as well as between the groups that had received oral BPQ versus oral ATQ. Furthermore, the difference between the negative control group and the group that had received the aerosolized placebo formulation was also not significant.

Bis-Benzimide stain

(a)

Diff-Quik stain

(b)

Figure 4-23: *Pneumocystis* **infection score as microscopically determined (magnification 200x) in lung impression smears stained with BB (a) and DQ (b).** Groups of 8 *P. murina*-infected RAG mice were treated as follows for 3 weeks (5 days a week) before sacrifice: 1 = untreated, 2 = 30 min exposure to aerosolized placebo dispersion, 3 = 20 mg BPQ nanosuspension/ kg mouse per os, 4 = 30 min exposure to aerosolized BPQ nanosuspension, 5 = 20 mg ATQ suspension/ kg mouse per os.

Figure 4-23b shows the infection scores obtained from the analysis of lung impression smears stained with DQ. The reference micrographs for estimating the infection rates for each mouse (0 to 4) were shown in Figure 3-15 in section 3.2.4.9.

The Kruskal-Wallis analysis of variance by ranks revealed a P value of 0.006, indicating a significant difference between the five groups compared. Multicomparisons made with the Dunn's post-Hoc test showed no significant difference for almost all groups compared by pairs. A statistically significant diminution in the grade of infection was only observed when comparing the group treated with BPQ per os with that treated with aerosolized BPQ (P <0.05). When comparing Figure 4-23a and 4-23b, the plotted median values suggest a similar tendency. However, group 3 that had received BPQ per os showed a considerably higher infection score when DQ-stained preparations were analyzed than for BB-stained preparations. When looking at the DQ-stained preparations, the intensity of the stain seemed to vary substantially between the trophozoite nuclei in different clusters and between individual parasites.

Figures 4-24a and 4-24b show a comparison between DQ-stained clusters found in lung material from non-treated controls (Figure 4-24a, upper), with clusters observed in mice treated with BPQ per os (Figure 4-24a, lower). The differences were related to diffuse fluorescent clouds (probable rests of clusters) observed with BB-stain (Figure 4-24b, lower), and intact nucleic material stained with BB (Figure 4-24b, upper).

Although the enumeration of trophozoites and cysts with the DQ-stain was difficult, the stain was highly useful for obtaining a rapid overview of the infection status, as well as histopathological information. One reason why *P. murina* organisms could not be individually identified and counted accurately with the DQ stain may be the small size of trophozoites (small forms 1.5-2 µm, large forms 3-5 µm; nuclei about 0.5-1 µm). Furthermore, cysts and trophozoites tend to stick to each other, forming very large aggregates as observed in severely infected animals. Though serial dilution of lung homogenates improved the visibility of the parasites somewhat, it remained difficult to distinguish between trophozoites and cell debris present in the preparation. Furthermore, these options cannot be applied to lung impression smears.
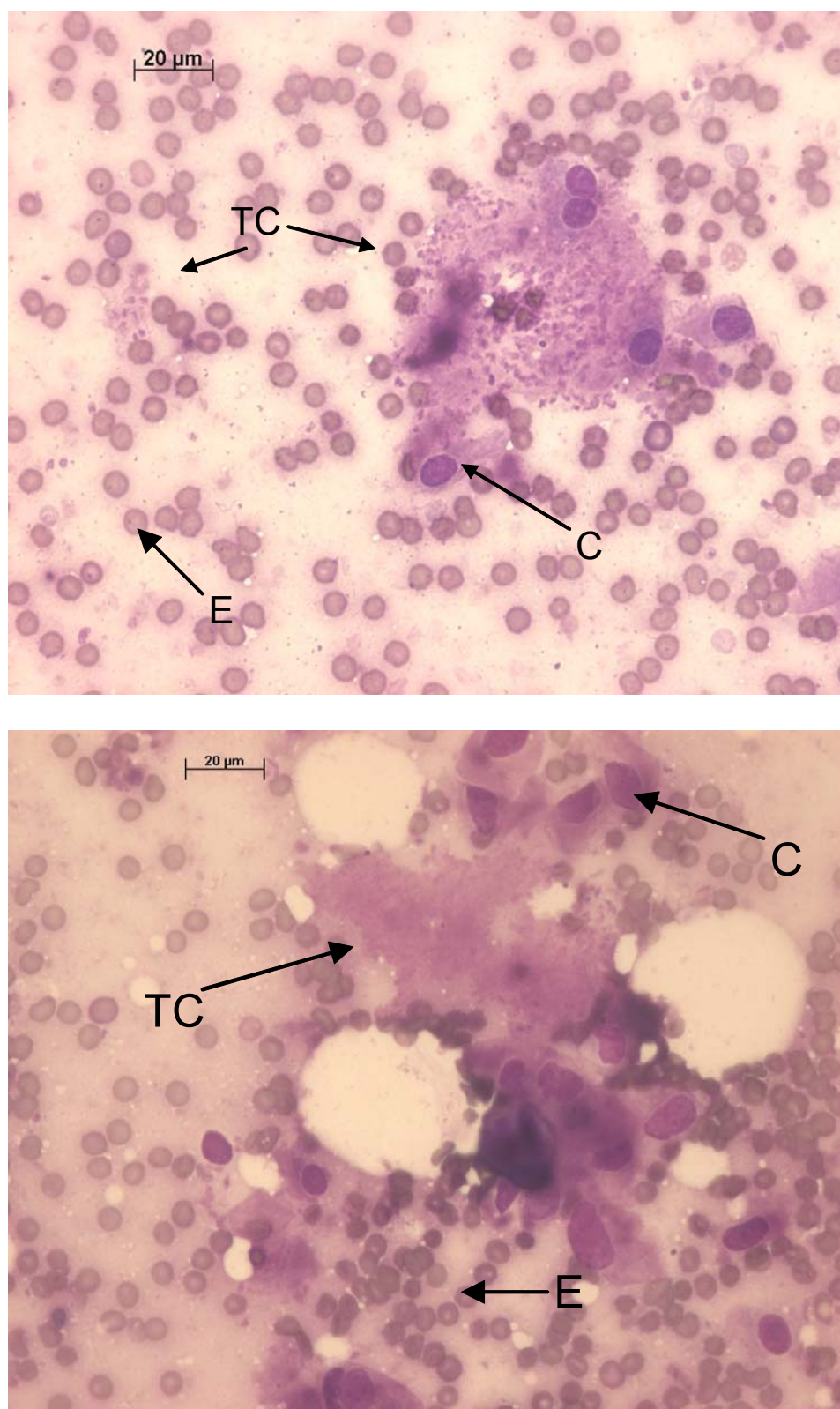
Figure 4-24a: Comparison between trophozoite clusters in lung impression smears stained with DQ. Infected animals were left untreated (upper) or were treated with BPQ per os (lower). Magnification 400x. Pictures show trophozoit clusters of the parasite (TC), erythrocytes (E) and host cells (C).
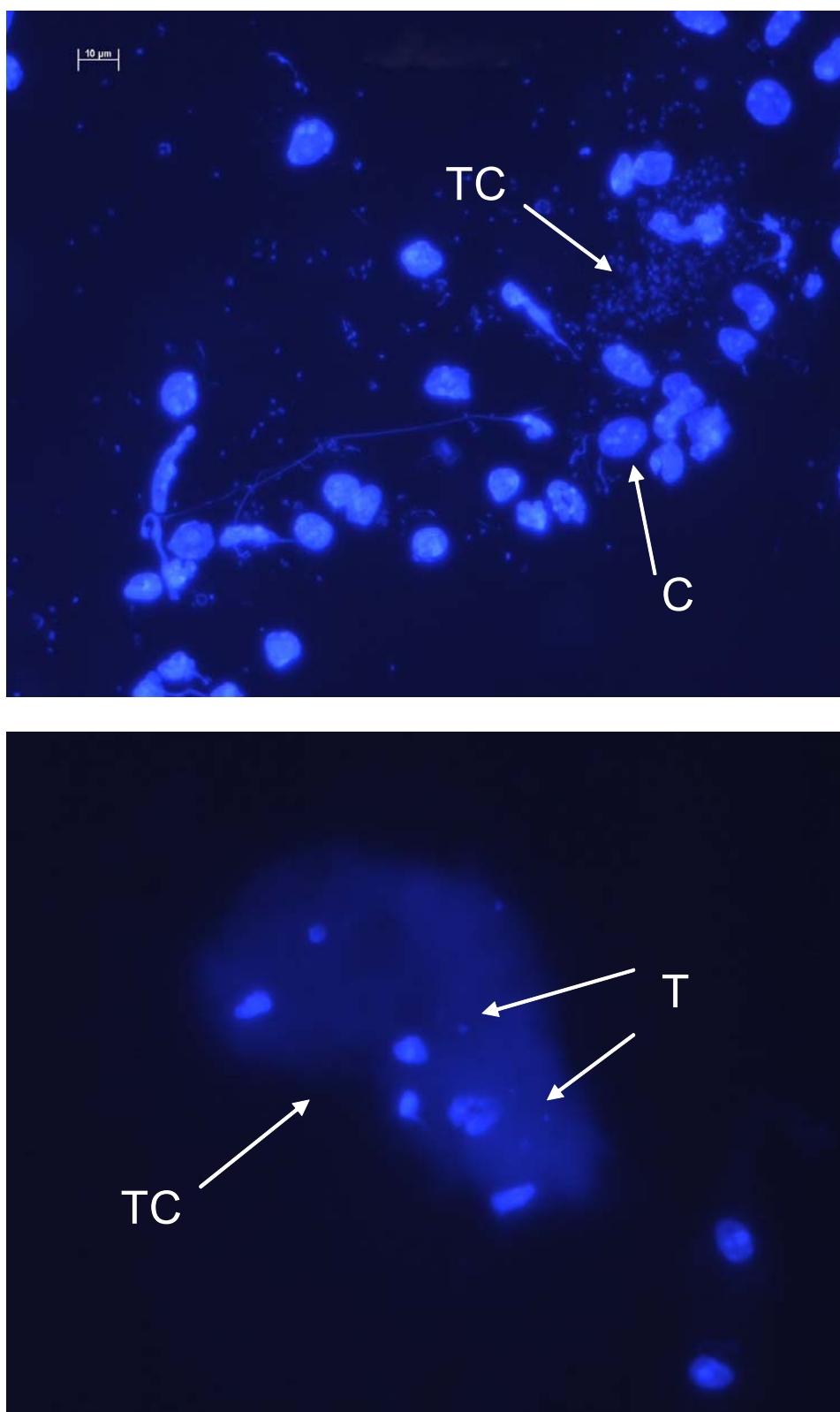
Figure 4-24b: Comparison between nuclei of trophozoite clusters in lung impression smears stained with BB. Infected animals were left untreated (upper) or were treated with BPQ per os (lower). Magnification 400x. Pictures show trophozoit clusters of the parasite (TC), host cells (C) and intact trophozoits (T).

Representative micrographs of DQ- and H&E-stained lung impression smears obtained from each of the experimental groups are shown in Figure 4-25. In general, the mice were only moderately infected when treatment was begun. Cysts were observed mainly along the walls of the alveoli. Later, individual parasites, small and large clusters of trophozoites were found, depending on the level of infection, i.e. the success of treatment. With progression of disease, the inter-alveolar spaces typically became filled with foamy, eosinophilic material and pulmonary macrophages. In most of the cases, the alveoli also contained individual parasites or clusters. Alveolar macrophages became considerably more prominent, and some multinucleated forms of granulocytes were also seen. The cytoplasm of macrophages became foamy and vacuolated, especially in those animals which had received BPQ as aerosol. In the H&E-stained micrographs, mice of groups 1 and 2 showed the thickened alveolar septa with hypertrophy and hyperplasia of the type II cells that is typical of progressed PcP. Both features appeared less prominent in mice from the treated groups 3 to 5. With the techniques applied here, it was not possible to distinguish if the macrophages accumulated primarily to remove *P. murina* parasites or the aerosol particles from the alveoli.
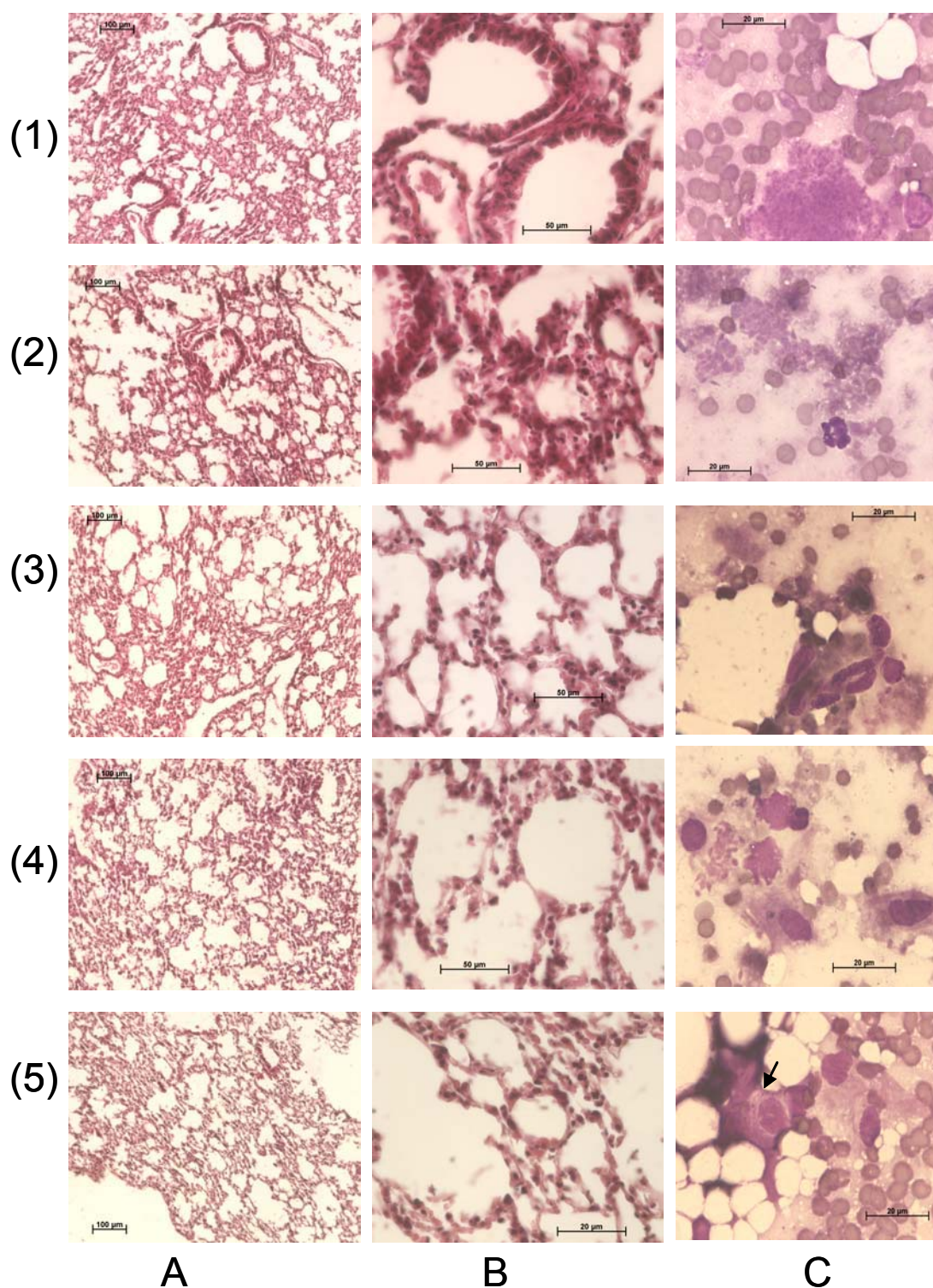
Figure 4-25: Details of lung morphology typically observed in *P. murina*-infected RAG mice after 3 weeks of therapy: untreated (1), 30 min exposure to aerosolized placebo dispersion (2), 20 mg BPQ nanosuspension/ kg mouse per os (3), 30 min exposure to aerosolized BPQ nanosuspension (4), 20 mg ATQ suspension/ kg mouse per os (5). Columns A and B show 100x respectively 400x magnifications of H&E-stained lung sections. Column C shows details of DQ-stained lung impression smears at 1000x magnification.

4.2.6 Conclusion

The use of aqueous dispersions containing drug nanocrystals is an easy and reliable option for the pulmonary delivery of poorly soluble drugs as has been shown here in a murine model for PcP. Considering the $\log_{10}$ parasite burden in lung homogenates, a reduction of the infection was seen with the drug buparvaquone. Most improvement was experienced when the drug was administered by means of a nebulizer device as part a whole-body inhalation system. Although improvements in the rate of infection were also seen in groups of mice treated orally with the buparvaquone nanosuspension, it needs to be considered that the dose of active drug reaching the lung with this inhalation model was in reality considerably lower than the dose available for absorption through oral administration. The oral administration of buparvaquone nanosuspension has demonstrated its effectiveness as a system enhancing bioavailability of this lipophilic drug. In the oral route, mice did not show a significant improvement relative to those which received oral atovaquone formulation (Wellvone®) used as a positive reference drug. This effect can be probably explained by the particle diameter of the microsuspension (d50% ~1µm). The particle size of the micronized atovaquone suspension is very close to the nanorange, so that the enhancement of bioavailability can be expected to be almost as strong as that from real nanosuspensions.

Rapid distribution, transport, and clearance of the drug nanocrystals were observed in a preliminary study with non-infected animals. Deposition of the drug nanocrystals in the lung parenchyma was low, which might be due to the size of the polydispersed aerosol reaching the animals, due to difficulties in the model used. The effective size of the aerosol is difficult to estimate, as the particle size may change from the nebulizer to the airways, for instance due to condensation of water vapour onto the droplets containing the drug in the high humidity environment in the lung. The use of aerosol delivery systems to test drugs targeting the lung is still an area of research that requires intensive development.

4.3. Nanocrystals in the solid state for pulmonary delivery

4.3.1 Preparation of the solid dispersions

All solid dispersion prepared had a drug load of 20 % (w/w). A summary of the solid dispersions produced is shown in Table 4-12.

Table 4-12 Summary of the composition and manufacture processes used in the preparation of the solid dispersions.

Batch identification	Production process	% w/w (solvent) buparvaquone	Sugar/polymer	% w/w (solvent) surgar or polymer
I-A-SFD	Spray-freeze drying	20 (TBA)	Inulin	80 (water)
I-B-SFD[**]	Spray-freeze drying	20 (TBA)	Inulin	80 (water)
I-NC-SFD	Spray-freeze drying	20 (water NS[*])	Inulin	70 (water)
I-NC-SD	Spray-drying	20 (water NS)	Inulin	70 (water)
PVP-A-SFD	Spray-freeze drying	20 (TBA)	PVP	80 (TBA)
PVP-B-SFD	Spray-freeze drying	20 (TBA)	PVP	80 (water)
PVP-NC-SFD	Spray-freeze drying	20 (water NS)	PVP	70 (water)
PVP-NC-SD	Spray-drying	20 (water NS)	PVP	70 (water)

[*] drug dispersed in aqueous poloxamer 188 surfactant solution as a nanosuspension

[**] Preparation based on TBA and inulin solution half concentrated from those used for batch I-A-SFD.

For the formulations based in BPQ nanosuspensions (NS), the concentration of the drug was 1% (w/w), dispersed in aqueous 0.5% poloxamer 188 solution using the same protocol of production as described in section 3.2.1.2 (page 52). The particle diameter of the nanocrystals is summarized in Table 4-13.

Table 4-13: Particle diameter values measured with PCS and LD. Aqueous dispersion of drug nanocrystals were stabilized adding 0.5 % poloxamer 188.
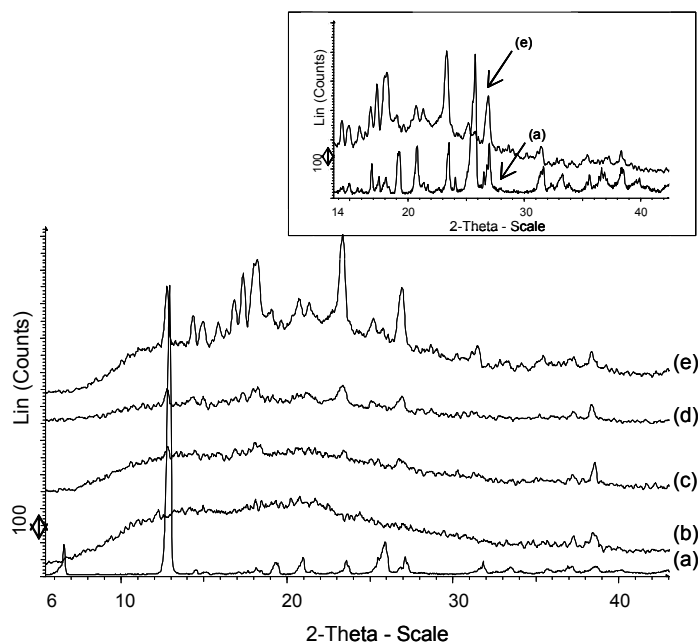
Size parameter	Formulation
PCS average diameter (nm)	465,8 ± 15.9
PCS Polydispersity Index	0,33 ± 0.05
d50% (µm)	0,70 ± 0.00
d90% (µm)	1,32 ± 0.02
d95% (µm)	1,50 ± 0.01
d99% (µm)	1,81 ± 0.00

Batch **I-A-SFD** was prepared as follows. A solution of BPQ in TBA (6.7 mg/mL w/w) and a solution of inulin in water (35.6 mg/mL w/w) were prepared at 50°C. These solutions were mixed at a volume ratio TBA/water 4:3 at a stirring rate of 300 rpm. The resulting homogeneous mixture was then immediately sprayed-freeze dried. Batch **I-B-SFD** was produced exactly as I-A-SFD, except that the starting solutions containing the drug and the carrier had only one half of the solids content present in the first batch. The PVP based solid dispersion **PVP-A-SFD** was produced by spray freeze drying a solution of drug and carrier in pure TBA. Solid dispersion **PVP-B-SFD** was produced by a similar procedure as I-A-SFD except that PVP was dissolved in water instead of inulin. A volume of NS was mixed at a ratio 1:1 with a carrier solution (inulin or PVP) and immediately spray-freeze dried. The inulin and PVP dispersions prepared with this procedure, were identified as **I-NC-SFD** and **PVP-NC-SFD** respectively. A similar sample preparation was followed in order to produce the batches **I-NC-SD** and **PVP-NC-SD**, except that the solid dispersions were prepared by spray drying instead of spray freeze drying.
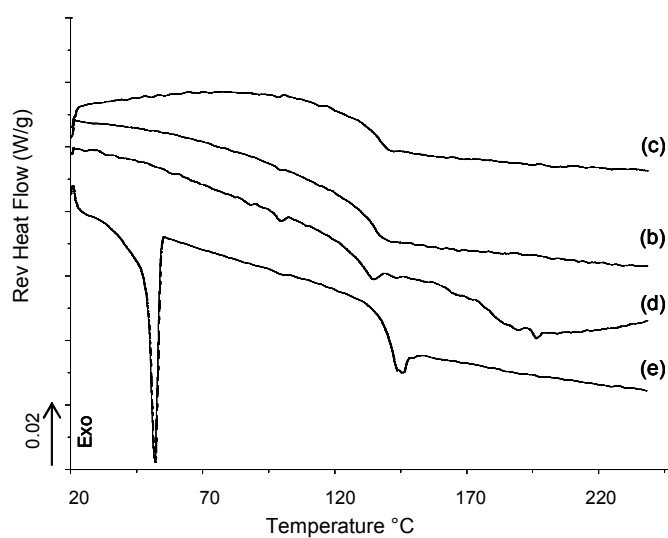
4.3.2 Degree of crystallinity and thermodynamical characteristics of the powders

The qualitative degree of crystallinity was determined with XRPD for all the formulations. During crystallisation the molecules rearrange themselves into an ordered array crystal lattice resulting in the decline of free energy of the system. It is therefore, generally expected that a system with a lower degree of crystallinity (amorphous), will have increased intrinsical energy due to solubilization of the components and lead to an improved solubility and rate of dissolution of the drug-polymer solid solution. The Fig. 4-26a presents the X-ray diffractograms of the PVP based powders compared with the original signals of the crystalline pure BPQ. The most amorphous sample is the solid dispersion prepared from TBA drug and polymer solutions PVP-A-SFD, followed by the sample PVP-B-SFD, where the polymer was dissolved in water. The sample containing nanocrystals prepared by SFD (PVP-NC-SFD) showed less signal intensity than the same formulation prepared by spray drying (PVP-NC-SD). Although the content of water in both samples was not determined, it could explain the difference in signal intensity, as the degree of crystallinity would be expected to be the same for samples produced with both processes. Amorphous drug was favoured by the antinucleating effect of poloxamer 188 and PVP.

The Fig. 4-26b nicely represents the transition temperature (T_g') of these PVP dispersions. The reversing heat flow signal of the MDSC measurement was used to determine the T_g' values (Weuts, Kempen et al. 2004). This value indicates polymer changes from the glassy to a rubbery state. In general terms, according to the Taylor-Gordon calculation (Gordon and Taylor 1952), the glass transition temperature of a multicomponent amorphous system can be roughly predictable from the T_g' and the weight fraction of the individual components, assuming no specific interactions between the components. A system where the polymer is considered to be miscible with the drug presents only one glass transition temperature, at an intermediate value between the T_g' of drug and polymer or polymer mixture. In the Fig. 4-26b the thermograms (b) and (c) corresponding to the solid dispersions PVP-A-SFD and PVP-B-SFD show only one T_g' at values 134.5 and 136.9 °C respectively. The T_g' of

(a)

(b)

Figure 4-26: Crystallinity and grade of miscibility investigations for PVP solid dispersions/solutions prepared with BPQ. (a) XRPD of the powders and (b) Thermograms obtained with MDSC showing the T_g values in the reverse heat flow signal. Sample identification is the same in both graphs: (a) Original crystalline BPQ powder; (b) PVP-A-SFD; (c) PVP-B-SFD; (d) PVP-NC-SFD; (e) PVP-NC-SD.

a mixture containing 80 % (w/w) PVP and 20 % BPQ could be found around 142 °C, therefore the reduction of the values is a clear indication of the blend of the polymer with the drug at the proportion mixed. The reduction of the T_g' value is due to the incorporation of a drug with a low molecular weight as BPQ (326 g/mol) which increases the grade of freedom of the polymer chain segments, acting as a plasticizer (Chokshi, Sandhu et al. 2005). On the other hand, the batch PVP-NC-SD (thermogram (e), Figure 4-26b), shows a T_g' of 142.1 °C with a less relaxed structure as the SFD product as indicated by a ∆Cp value of 463.1 mJ/g/°C. The non-reduced T_g' value of PVP, as well as the melting endotherms observed in the total heat flow signal, confirmed the crystalline state for the drug and poloxamer 188, which were encapsulated by a PVP layer during the SD process, having the drug a separated phase within the carrier, but being not necessarily an interacting molecularly with it.

The MDSC experiments performed here, total amorphous state or degree of crystallinity of the samples PVP-A-SFD and PVP-B-SFD could be confirmed. The complete disappearance of the melting endotherm of the drug in the total heat signal flow signal of the MDSC measurement can indicate a complete amorphous state of the drug and poloxamer 188 by association with PVP. However, MDSC scanning process of these samples could also have originated the fusion of the PVP, conducing to the dissolution of BPQ and a false information of crystallinity of the samples investigated. Therefore, it was considered important a confirmation through XRPD technique.

Diffractograms shown in Figure 4-26a demonstrate the reduced crystallinity of samples PVP-A-SFD and PVP-B-SFD. The crystallinity of the samples was confirmed for samples containing nanocrystals. The diffraction pattern of sample PVP-NC-SD could be perfectly associated to the diffraction pattern of the original powder (see Figure 4-26a, zoom).

The XRPD of inulin solid dispersions can be seen in Figure 4-27. As expected, the degree of crystallinity of the samples I-A-SFD and I-B-SFD was very similar (curves (c) and (d)) and both as crystalline as the sample prepared from drug nanocrystals I-NC-SFD. The grade of crystallisation in the original nanosuspension can be seen in curve (e). The improved dissolution of drug nanocrystals prepared by HPH is not only favoured by an increase in surface area, but also due to reduced drug crystallinity.
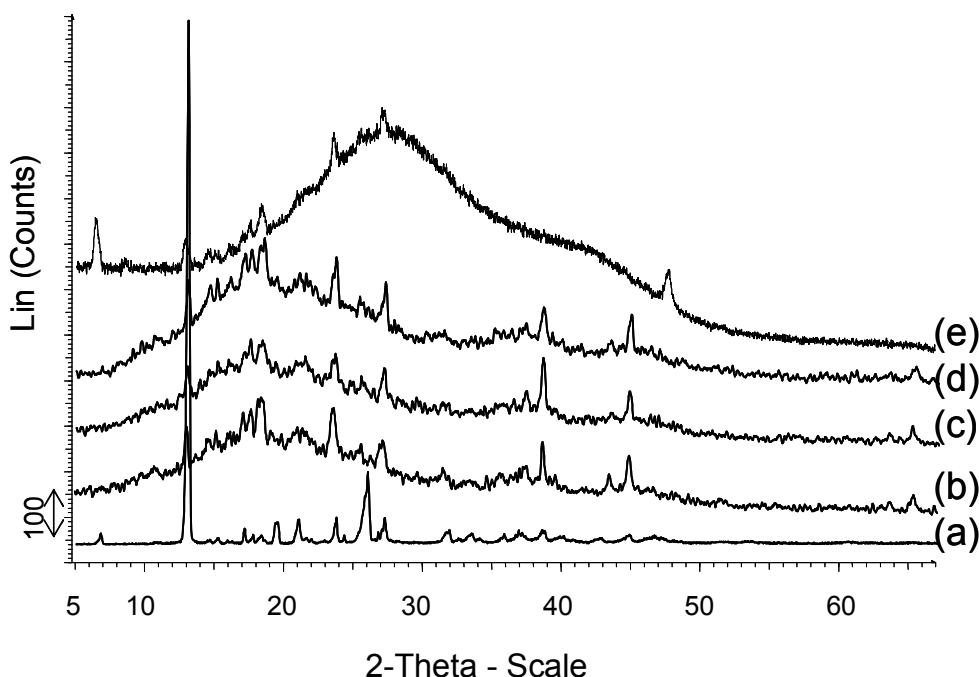
Figure 4-27: XRPD studies of BPQ incorporated into inulin solid dispersions.
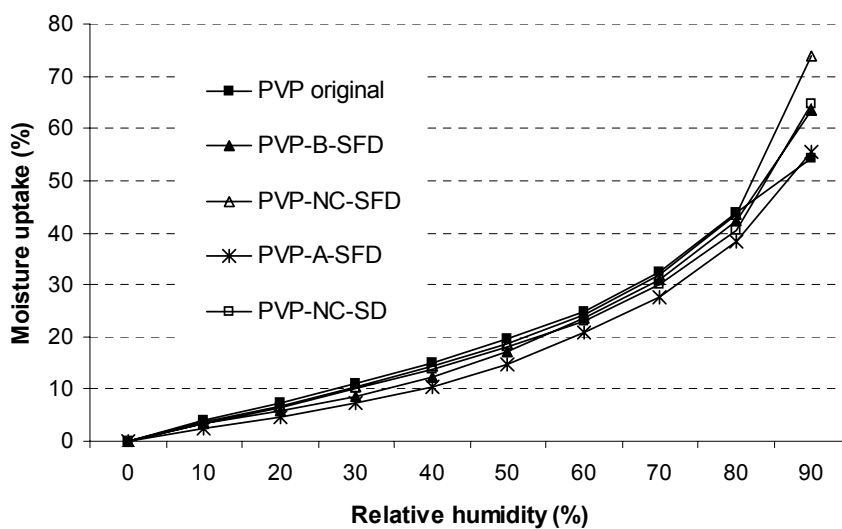Samples are labelled as follows: (a) Original crystalline BPQ powder; (b) I-NC-SFD; (c) I-A-SFD; (d) I-B-SFD; (e) Original BPQ nanosuspension in liquid state.

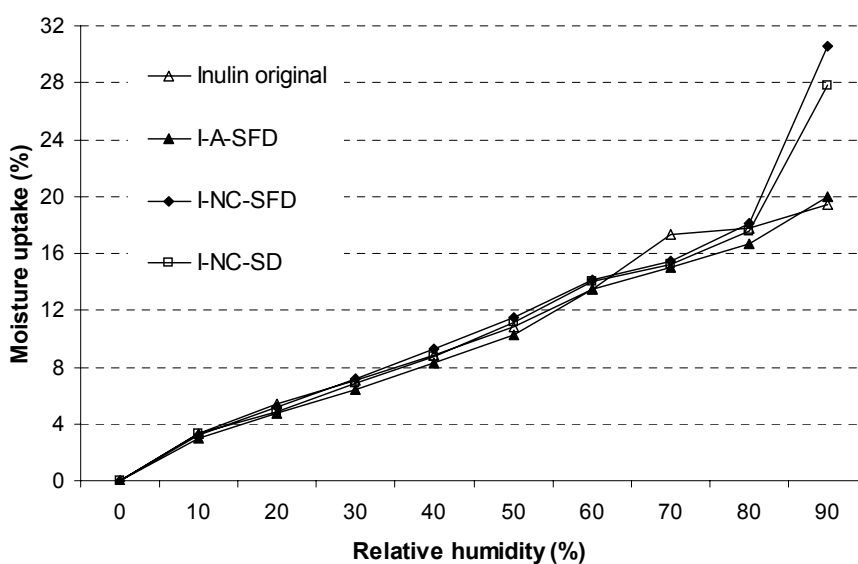## 4.3.3 Water vapour absorption into solid dispersions/solutions

Amorphous materials absorb water vapours in large amounts relative to the corresponding crystalline state. Molecules in an amorphous phase are capable of absorbing water vapour into the solid bulk in addition to surface adsorption during a similar sorption cycle and conditions (Crowley and Zografi 2002). The Figure 4-28 represents the percentage moisture uptake observed in the PVP and inulin powders prepared.

Assuming that the moisture uptake by BPQ is negligible, the measured data were divided by 0.8 or 0.7, according to the case (one minus the drug fraction). When the drug is molecularly distributed over the carrier and when the drug interacts with the carrier, it is expected that the uptake of water by the carrier will be reduced (hydrophobization of the hydrophilic carrier by the lipophilic drug (van Drooge,

Hinrichs et al. 2006). BPQ is expected to interact with PVP. An effect of incorporation of BPQ on the uptake of water cannot be recognizable in most of the samples (except for PVP-A-SFD, but the effect is negligible). These results indicate that BPQ is incorporated as particles and not molecularly incorporated in the polymer. PVP original powder and the solid dispersions prepared with PVP absorbed around 40% of moisture at a relative humidity of 80%. The inulin powders, where the drug was mainly rearranged in a micro- or nano-crystalline structure absorbed around 16% of moisture at the same relative humidity value, as the inulin original powder. Samples based in nanosuspension formulation, showed a DVS pattern confirming the presence of nanoparticles in the carrier but not incorporated in the molecular level, showing a very similar moisture uptake than that observed for the PVP powder alone. These results confirmed the previous observations in X-Ray diffraction patterns.

(a)

(b)

Figure 4-28: Dynamic vapour sorption (DVS) studies of the BPQ powders prepared with carrier PVP (a) and inulin (b). The plots compare the percentage of moisture uptake of the powders formulated with that of the original carrier. The moisture absorption cycle was performed in a range from 0 to 90% RH.

4.3.4 Morphology and structure of the powders

The Figures 4-29a to 4-29h show the SEM photographs taken from inulin and PVP powders of BPQ prepared using different processes. Spray freeze dried particles showed mostly spherical shape, with different grades of aggregation. With SEM (7500 x magnification) it can be seen for the sample I-A-SFD (Figure 4-29a) that the structures formed are spherical (size distribution ~ 1-30 μm, mean particle size ~9 μm, as measured by laser diffraction with Rodos system at 1 bar). These hollow spheres are porous as typical product from spray freeze drying process. The porous surface structure of these particles is a remainder of the small ice crystals formation within the small frozen droplets due to supercooling (Sonner, Maa et al. 2002; Yu, Rogers et al. 2002). It was possible to distinguish the very small crystals (size distribution <1-10 μm) incorporated between the sugar net (indicated in the photograph with an arrow). A very logical explanation for that is that the extremely low solubility of the drug in water, favoured the recrystallisation of the drug during the process when the saturated TBA drug solution was mixed with the polymer aqueous solution.
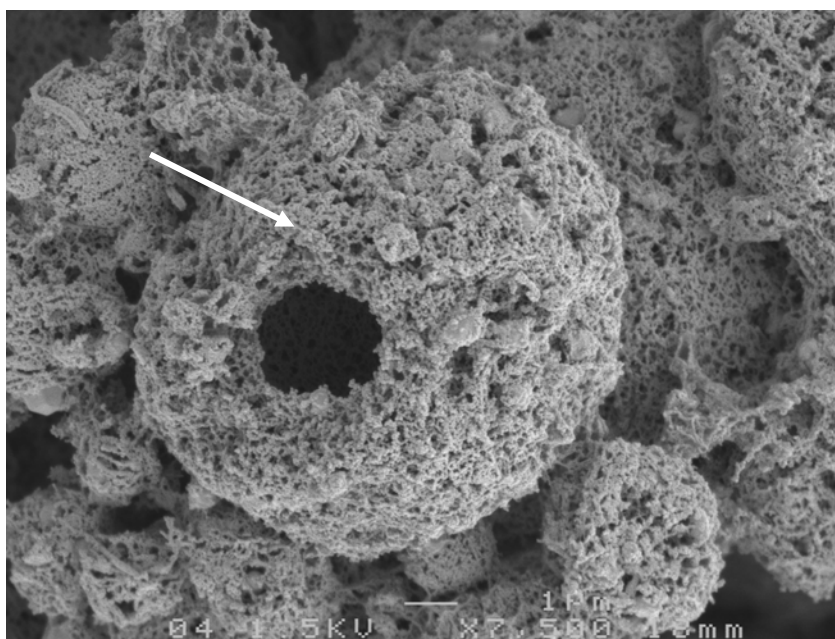

Figure 4-29a: SEM picture of the buparvaquone powder particles in the sample I-A-SFD. A mixture of TBA drug solution and aqueous inulin solution was spray-freeze dried. Hollow particles were formed with small nanocrystals incorporated between the sugar net (arrow). Magnification 7500 x.

The morphology of the sample I-B-SFD (Figure 4-29b) presented a very similar physical structure as I-A-SFD. The SEM photo indicated the formation of drug crystals although the concentration of the solutions mixed was only one half of the previous sample. Further reasons besides the apparent supersaturation of the drug and inulin solutions are responsible for the presence of crystals. The freezing step during the lyophilization of the product should be considered for explanation. The mixture of the drug with water probably reached the eutectic crystallisation temperature or the rate of freezing was slow for this mixture, supporting the crystallisation. Although crystals are present, an increase in dissolution can be predicted, as the crystals size distribution seems to be as small as that seen in the first batch.
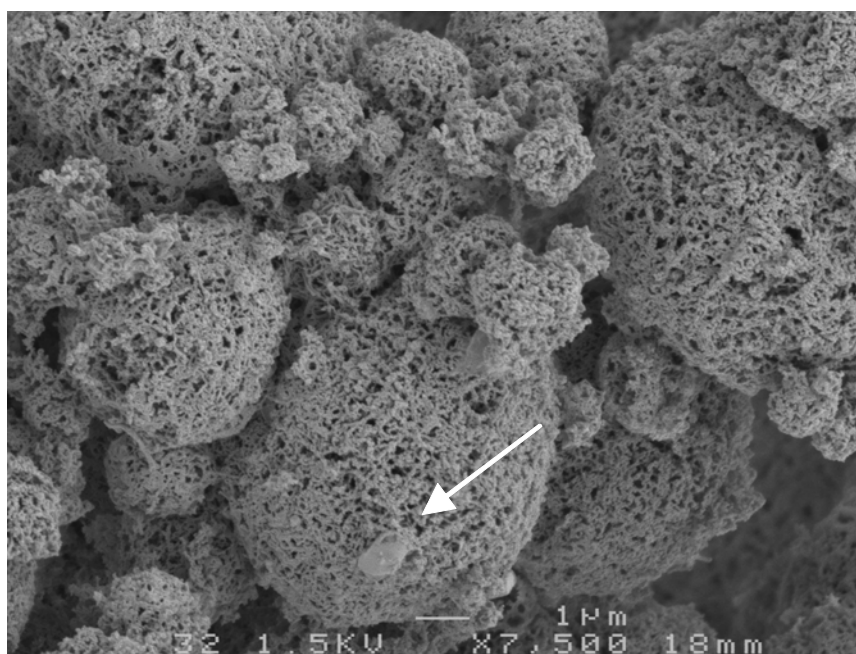

Figure 4-29b: SEM picture of the buparvaquone powder particles in the sample I-B-SFD. A half diluted mixture of TBA drug solution and aqueous inulin solution was spray-freeze dried. Hollow particles were formed with small nanocrystals incorporated between the sugar net (arrow). Magnification 7500 x.

The powder PVP-A-SFD presented a sponge-like appearance. The internal structure (Figure 4-29c) seems to form a phase separated solid dispersion. Particles formed are spherical but not hollow and the highly porous structure of the polymer is distinguished only internally in the particles. The net of the polymer chains was arranged independently from a coating layer involving the polymer, which could be constituted of drug molecules.
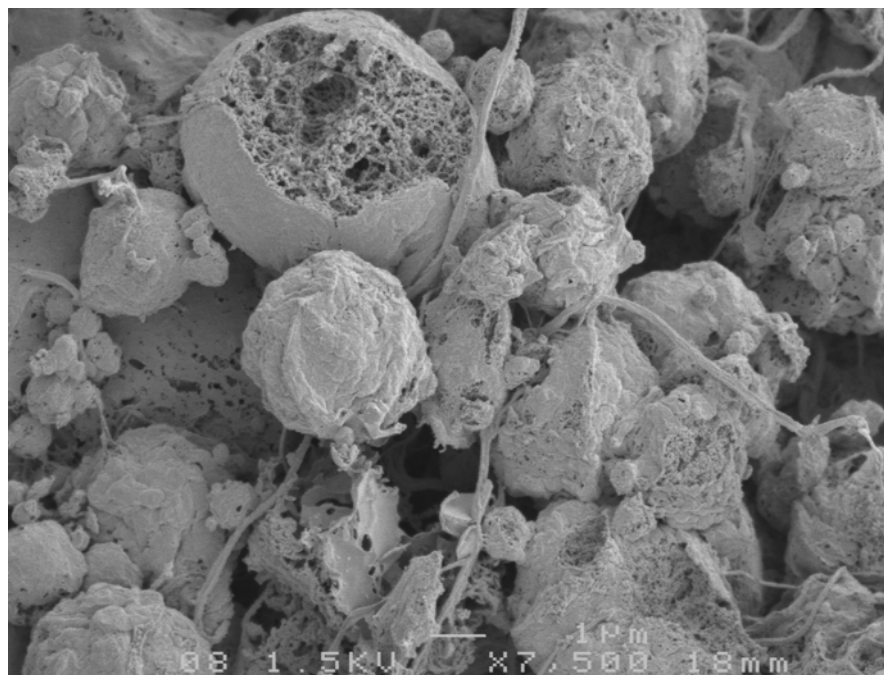

Figure 4-29c: SEM picture of the buparvaquone powder particles in the sample PVP-A-SFD. A mixture of TBA drug solution and TBA solution of PVP was spray-freeze dried. Sponge-like particles were formed. Magnification 7500 x.

The sample PVP-B-SFD shows a more homogenious distribution of the drug in the polymer. No separation of phases can be distinguished. Irregular forms on the surface of the particle due to polymer arrangement can be seen in the SEM picture shown in Figure 4-29d.
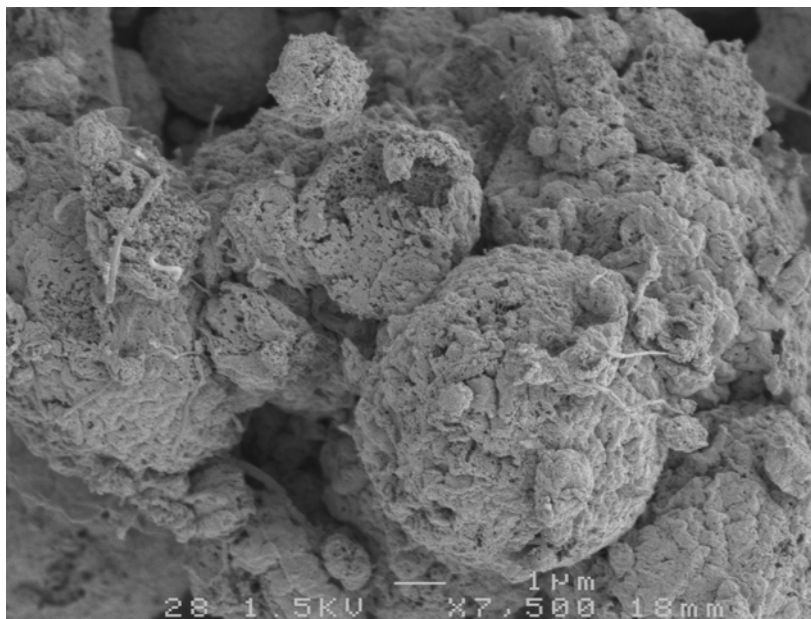
Figure 4-29d: SEM picture of the buparvaquone powder particles in the sample PVP-B-SFD. A mixture of TBA drug solution and aqueous solution of PVP was spray-freeze dryed. Highly porous particles were formed. Magnification 7500 x.

Nanocrystals were incorporated in particles produced using inulin as carrier. The structure of the sample I-NC-SFD can be seen in Figure 4-29e. The size of the powder resultant from the spray freeze drying process had a size distribution in the range from 2-50 µm and an average size of 16 µm (measured by laser diffraction Rodos system, 1 bar). The particles do not show a spherical structure, but it is possible to distinguish the presence of the drug nanocrystals allocated between the inulin structures. The starting concentration of the inulin/nanosuspension aqueous mixture was relatively low (2.5% w/w), that involves the growth of ice crystals, which constitutes most of the droplets composition during the freezing step of the lyophilization, explaining the high porosity observed. As water left the liquid specimens, the surface tension increased, this could explain the collapse of droplets under this tension, if those structures were of high fragility. The components in this mixture, BPQ, poloxamer 188 and inulin formed aggregates of undefined structure, organised in separated solid phases.
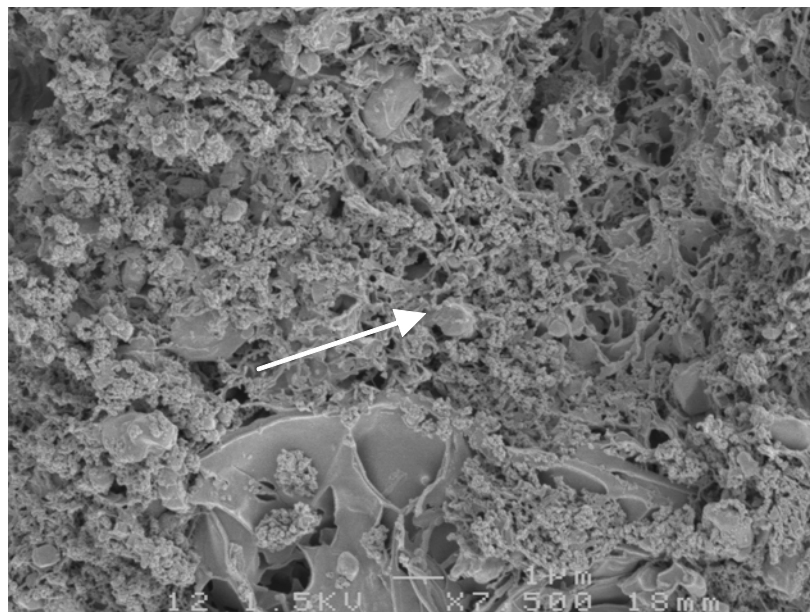
Figure 4-29e: SEM picture of the buparvaquone powder particles in the sample I-NC-SFD. A mixture of BPQ nanosuspension and aqueous solution of inulin was spray-freeze dryed. Aggregates of undefined structure were formed. Drug nanocrystals can be distinguished (arrow). Magnification 7500 x.

A totally different rearrangement was observed for the sample including PVP as carrier. The structure of the sample PVP-NC-SFD is shown in Figure 4-29f. Porous spherical particles were formed. A better interaction of the PVP and poloxamer 188 structures wetting the drug, could also conduct to a more stable rearrangement. Although the concentration of the nanosuspension atomized was the same as the previous sample, the presence of PVP in the formulation produced a further reduction of the surface tension probably due to formation of PVP-poloxamer complexes during the freezing process. This situation and the increase in the viscosity during the process allowed the droplets to keep the spherical form.
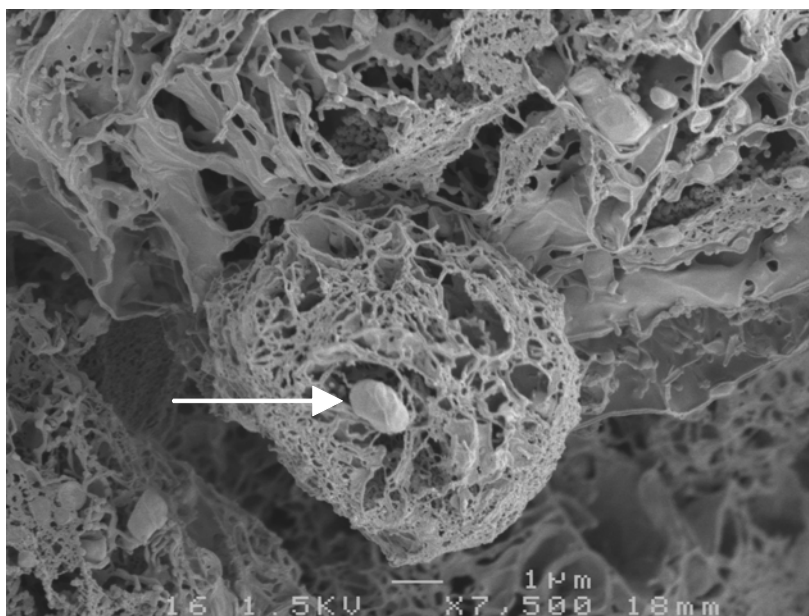
Figure 4-29f: SEM picture of the buparvaquone powder particles in the sample PVP-NC-SFD. A mixture of BPQ nanosuspension and aqueous solution of PVP was spray-freeze dried. Porous spherical particles were formed. Drug nanocrystals can be distinguished (arrow). Magnification 7500 x.

Formulations with nanocrystals stabilized with poloxamer 188 and inulin/PVP as carrier were spray dried producing powders with a very different structure. The particles can be seen in Figures 4-29g and 4-29h. Inulin based particles (sample I-NC-SD) showed a smooth surface, organised as big aggregates. The sample PVP-NC-SD in the other hand shows also smooth surface but shrinkage due to evaporative water loss during SD process. This is a known phenomenon when particles are prepared from low concentrated solutions, due to low particle strength. An increase of the surface activity in the aqueous solution, due to reduction of surface tension can also lead to particles shrinkage.
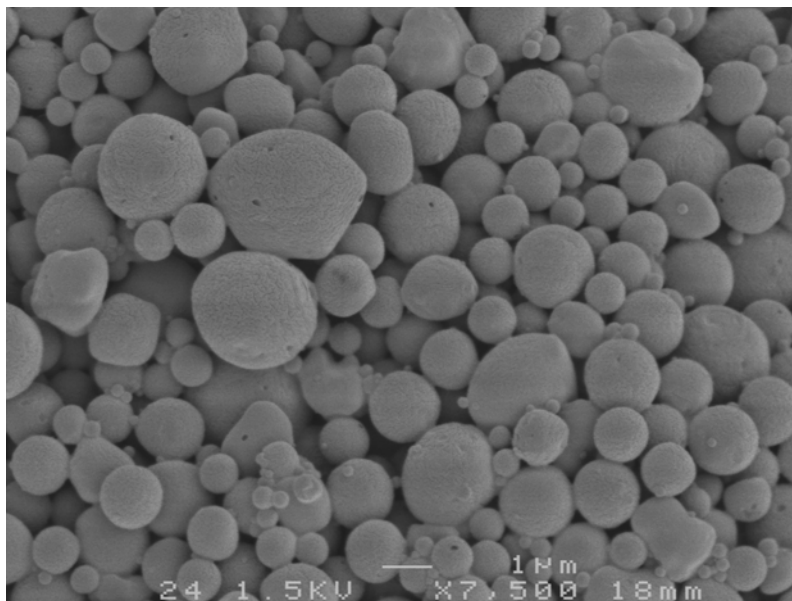
Figure 4-29g: SEM picture of the buparvaquone powder particles in the sample I-NC-SD. A mixture of BPQ nanosuspension and aqueous solution of inulin was spray dried. Rounded particles were formed. Magnification 7500 x.
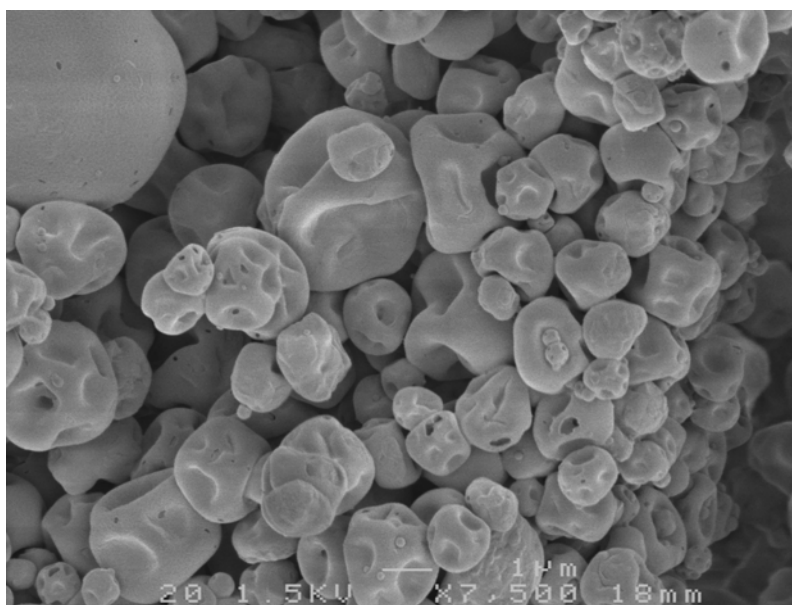

Figure 4-29h: SEM picture of the buparvaquone powder particles in the sample PVP-NC-SD. A mixture of BPQ nanosuspension and aqueous solution of PVP was spray dried. Shrinkage particles were formed. Magnification 7500 x.

4.3.4 Dissolution behaviour: Mechanisms of drug release

The Figure 4-30 shows the dissolution profile obtained within one hour of the solid solutions/dispersions using PVP as carrier. As expected, the dissolution of the non-formulated BPQ was extremely low. Around 3% of the drug original crystals were dissolved after one hour and only 12% after the 5 hours monitored.
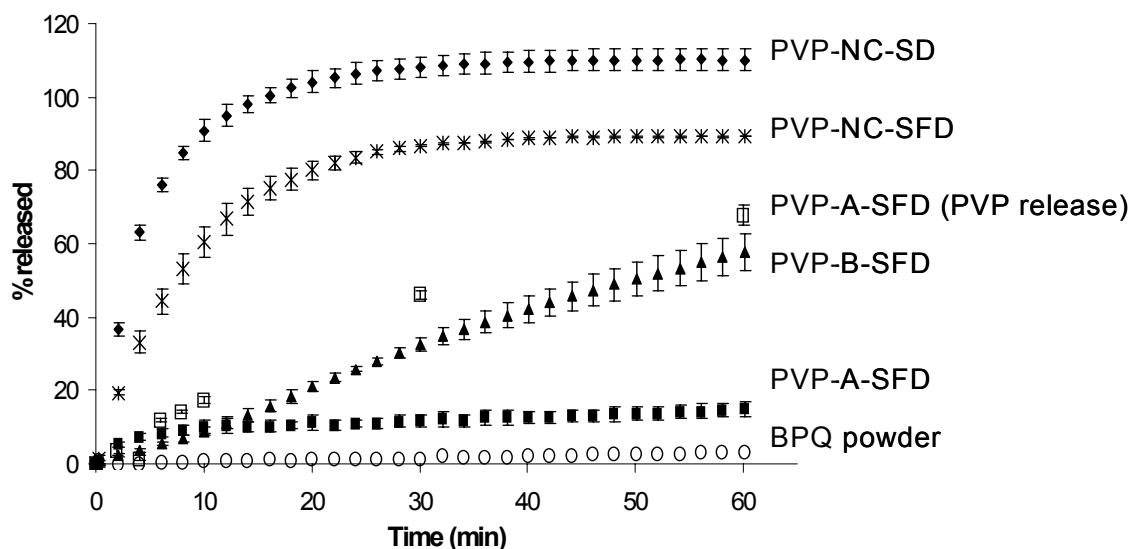

Figure 4-30: BPQ release curves of the PVP powders prepared. Dissolution was tested using the USP Apparatus II, and 2% Tween solution as dissolution medium (rotating basket method). PVP release in water from sample PVP-A-SFD is also plotted for reference.

The lowest rate of dissolution of the BPQ formulations was observed for the less amorphous sample and increased with the crystallinity grade of the powders. According to XRPD and MDSC results, the sample PVP-A-SFD the drug is incorporated in the polymer in a partially amorphous state, which according to the dissolution behaviour observed, either the amorphous particles are forming big aggregates, or are probably too large, slowing down the rate of dissolution. The Figure 4-30 shows that only 15% of the drug was released after 1 hour. 64% of BPQ was released after 6 hours and 90% after 21 hours. The slow dissolution of the drug powder was attributed to the poor wetting ability of the powder particles, as mentioned before, due to too large particles. During the first minutes of dissolution,

the powder floated on the surface of the medium, indicating a lipophilic nature of the particles surface probable due to orientation of drug molecules towards the surface of the powders. Although the disintegration of the powder particles was seen in the dissolution baskets, the percentage of drug release detected was extremely low. In order to further investigate the dissolution behaviour of this powder, the release of PVP was quantified. PVP showed a similar dissolution profile as the BPQ formulated in the sample PVP-B-SFD, where the polymer was dissolved in water instead of TBA during the production process. These results indicated that in the last sample (PVP-B-SFD), the drug release was controlled by the PVP dissolution, that means, a carrier controlled dissolution. Once in contact with the dissolution medium, the drug particles de-aggregated, yielding separated drug and polymer entities in the dissolution beaker. The drug dissolved very slowly very probably due to its surface area. The polymer molecules dissolved faster, but did not influence the drug release for a faster dissolution (hydrophobisation effect). As the presence of water in the production of samples PVP-A-SFD and PVP-B-SFD strongly influenced the dissolution of the drug, strong electrostatic interactions such as dipole-dipole interaction or H-bonding interaction very probably improved drug-polymer associations. (e.g. interaction between carboxyl (COO-) and HOH or NH- and COO- groups). The interaction between PVP-30 and other 1,4-napthoquinone has been reported before. It has been suggest that drug-polymer interaction probably occurs via intermolecular hydrogen bonding between the drug hydroxyl and polymer carbonyl groups (Granero and Longhi 2002). Therefore, the presence of HOH groups may build strong bridges for interaction between both structures.

The dissolution of sample PVP-B-SFD is slower than sample PVP-NC-SFD. The powders produced by SD process, where the drug nanocrystals are inside encapsulated by the polymer film but remain crystalline and phase separated, showed an even faster rate of dissolution, depending only on the drug size. Additionally, poloxamer 188 as a wetting agent can increase the release rate significantly, not only reducing the aggregation of the dispersed particles, but also acting as a binder with the PVP chains. Furthermore, SEM studies showed that the powders prepared from nanosuspensions by SFD are more porous, also facilitating hydration and dissolution. In both PVP samples (PVP-NC-SFD and PVP-NC-SD), once the solid dispersion was exposed to aqueous media and the carrier dissolved,

the drug was released as very fine nanoparticles, increasing surface area and dissolution rate.

The Figure 4-31 represents the release profile of the solid dispersions based in inulin as carrier. The dissolution behaviour of the BPQ original powder and liquid nanosuspension are shown for comparison.
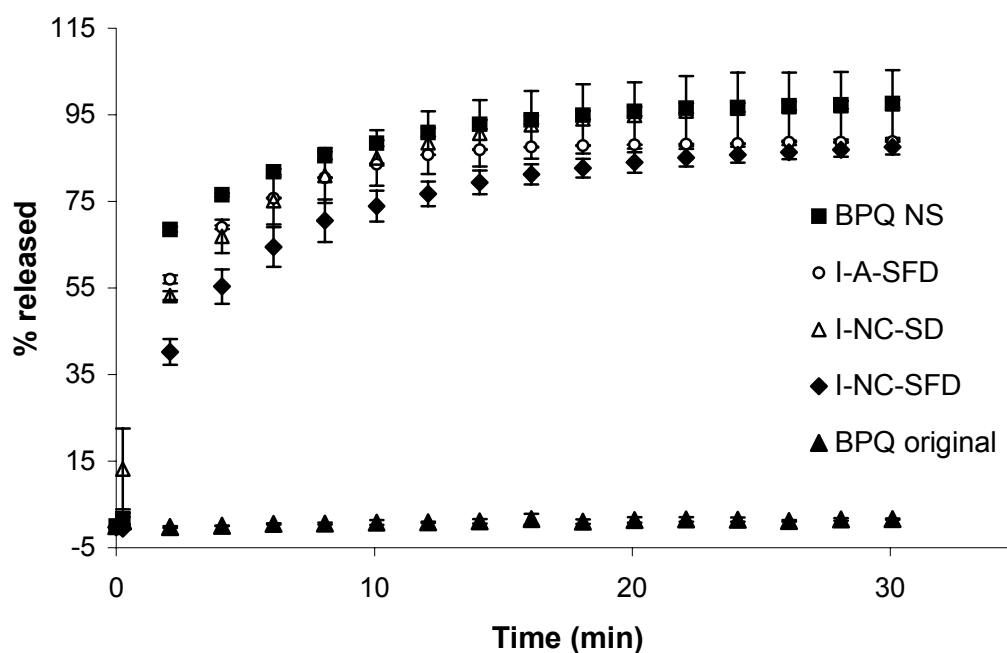

Figure 4-31: BPQ release curves of the inulin powders prepared. Dissolution was tested using the USP Apparatus I, and 2% Tween solution as dissolution medium. BPQ NS identify the original buparvaquone nanosuspension formulation.

All formulations improved the rate of release of the drug drastically, showing in all cases at least 75% of the drug released after 20 min. The fastest dissolution observed for the samples I-NC-SD and I-A-SFD which was almost identical although they were produced with very different processes. Both samples had a dissolution mechanism carrier controlled and the drug incorporated as nanocrystals. From the dissolution rate profile of sample I-A-SFD, it can be assumed that the size of the nanocrystals formed in the sample, was very similar than the nanosuspension based powder. While the sample I-NC-SD may be favoured for dissolution by the presence of poloxamer 188 in the formulation, the sample I-A-SFD formed hollow porous particles, conducing to an instant dissolution of the inulin in the dissolution medium

and dissolution of the small drug crystals contained. A relatively slower release profile is shown by sample I-NC-SFD. This can be explained by the big and irregular powder aggregates seen in SEM studies.

Both methodologies used here for the preparation of solid dispersions yielded products with improved rate of dissolution. The route to produce solid dispersions by spray freeze drying a TBA drug solution mixed with an aqueous matrix material solution is of fast and very practical use. However, for small molecules with a very low T_g' just as BPQ, spontaneous crystallization can occur especially when the drug amount is larger than the solubility limit in inulin. Even when crystals formed small enough to lead to an improvement in dissolution, the reproducibility of crystallization and size distribution of the crystals formed can show difficulties to be controlled. Drug loading in these dispersions is therefore limited and must be analysed for each drug-carrier combination selected.

4.3.6 Conclusion

The second route of producing solid dispersions including drug nanocrystals into porous particles (spray freeze drying) or non-porous particles (spray drying) showed a very fast dissolution of the drug, with a mechanism of dissolution dependent on the size of the drug and the wettability of the particles achieved during the homogenisation process. The fact that the drug is in a size controlled crystalline state is also an advantageous approach, having the disadvantage of the relatively more time consuming and sophisticated technology for the production of the drug nanocrystals. A crystalline product in these solid dispersions can reward on stability advantages and higher drug loading capacities.